© 2014. Published by The Company of Biologists Ltd | Journal of Cell Science (2014) 127, 3024–3038 doi:10.1242/jcs.136150

RESEARCH ARTICLE

Metabolism and mis-metabolism of the neuropathological signature protein TDP-43

Chi-Chen Huang[1,2,‡], Jayarama Krishnan Bose[1], Pritha Majumder[1], Kuen-Haur Lee[3], Jen-Tse Joseph Huang[4], Jeffrey K. Huang[5] and Che-Kun James Shen[1,2,‡]

ABSTRACT

TDP-43 (also known as TARDBP) is a pathological signature protein of neurodegenerative diseases, with TDP-43 proteinopathies including frontotemporal lobar degeneration (FTLD)-TDP and amyotrophic lateral sclerosis (ALS)-TDP. These TDP-43 proteinopathies are characterized by cytoplasmic insoluble TDP-43-positive aggregates in the diseased cells, the formation of which requires the seeding of TDP-25 fragment generated by caspase cleavage of TDP-43. We have investigated the metabolism and mis-metabolism of TDP-43 in cultured cells and found that endogenous and exogenously overexpressed TDP-43 is degraded not only by the ubiquitin proteasome system (UPS) and macroautophagy, but also by the chaperone-mediated autophagy (CMA) mediated through an interaction between Hsc70 (also known as HSPA8) and ubiquitylated TDP-43. Furthermore, proteolytic cleavage of TDP-43 by caspase(s) is a necessary intermediate step for degradation of the majority of the TDP-43 protein, with the TDP-25 and TDP-35 fragments being the main substrates. Finally, we have determined the threshold level of the TDP-25 fragment that is necessary for formation of the cytosolic TDP-43-positive aggregates in cells containing the full-length TDP-43 at an elevated level close to that found in patients with TDP-43 proteinopathies. A comprehensive model of the metabolism and mis-metabolism of TDP-43 in relation to these findings is presented.

KEY WORDS: TDP-43, Protein degradation, Proteolytic cleavage, Chaperone-mediated autophagy, TDP-43-positive aggregate, TDP-43 proteinopathies

INTRODUCTION

TAR DNA-binding protein (TDP-43, also known as TARDBP) is an RNA- and DNA-binding factor with multiple cellular functions (Baloh, 2011; Buratt et al., 2001; Chen-Plotkin et al., 2010; Cohen et al., 2011; Lagier-Tourenne et al., 2010; Lee et al., 2012; Wang et al., 2008). It has also been identified as the major component of the ubiquitylated inclusions (UBIs) in frontotemporal lobar degeneration (FTLD-U) and amyotrophic lateral sclerosis (ALS) (Arai et al., 2006; Cohen et al., 2011; Neumann et al., 2006). TDP-43 is ubiquitylated, hyperphosphorylated, cleaved into C-terminal fragments and redistributes from the nucleus to the cytoplasm (Arai et al., 2006; Hasegawa et al., 2011; Igaz et al., 2008; Neumann et al., 2006). The 25 kDa and 35 kDa TDP-43 fragments (known as TDP-25 and TDP-35, respectively) are generated mainly through caspase-3-mediated cleavage of TDP-43 (Zhang et al., 2007). The accumulation of TDP-43 within the insoluble UBIs suggests that mis-regulation of genes and/or factors involved in the processing and degradation of intracellular proteins likely contribute to TDP-43 proteinopathies and the associated pathology.

The formation of the TDP-43-positive UBI aggregates in TDP-43 proteinopathies reflect several other neurodegenerative diseases that are also characterized by protein aggregates (Bates, 2003; Hashimoto et al., 2003; Lansbury and Lashuel, 2006; Ross and Poirier, 2004; Ross and Poirier, 2005). A common characteristic of these diseases is the mis-metabolism of the signature proteins in the aggregates and/or inclusions [e.g. Htt in the Huntington's disease, α-synuclein in Parkinson's disease, β-amyloids in Alzheimer disease, etc. (Bates, 2003; Hashimoto et al., 2003; Ross and Poirier, 2004)]. To date, several studies have reported findings regarding the degradation of the TDP-43 protein. In particular, it has been found that overexpressed full-length TDP-43 protein and its truncated 25 kDa and 35 kDa fragments are degraded through both the ubiquitin proteasome system (UPS) (Kim et al., 2009; Urushitani et al., 2010; Wang et al., 2010) and macroautophagy pathways (Caccamo et al., 2009; Filimonenko et al., 2007; Ju et al., 2009; Wang et al., 2012). Most short-lived proteins are degraded by UPS through the 26S proteasome (DeMartino and Slaughter, 1999), whereas the autophagy–lysosomal pathway primarily catabolizes unnecessary organelles, long-lived proteins and misfolded and/or aggregated proteins (Ravikumar et al., 2010). However, ubiquitin-modified proteins can also be degraded through the autophagy–lysosomal system, which comprises macroautophagy, chaperone-mediated autophagy (CMA) and microautophagy (Kirkin et al., 2009; Welchman et al., 2005).

In contrast to for overexpressed TDP-43, relatively few studies have focused on the degradation pathways of the endogenous TDP-43 protein species. Among these studies, one immunofluorescence staining analysis has shown that depletion of functional multivesicular body (MVBs), required for the macroautophagy degradation pathway, results in the accumulation of the endogenous TDP-43 in the cytoplasm as ubiquitylated species (Filimonenko et al., 2007). In another study, overexpression of ubiquilin 1 (UBQLN), a proteasome-targeting factor, results in an increased amount of insoluble full-length TDP-43 protein and ubiquitylated aggregates consisting of endogenous TDP-43 with the autophagosomal marker LC3 (Kim et al., 2009). Notably, under normal conditions, the cellular concentration of the TDP-43 protein is autoregulated through a negative-feedback loop (Ayala et al.,

[1]Institute of Molecular Biology, Academia Sinica, Nankang, Taipei, Taiwan. [2]Graduate Institute of Neural Regenerative Medicine, College of Medical Science and Technology/Center for Neurotrauma and Neuroregeneration, Taipei Medical University, Taipei, Taiwan. [3]Graduate Institute of Cancer Biology and Drug Discovery, College of Medical Science and Technology, Taipei Medical University, Taipei, Taiwan. [4]Institute of Chemistry, Academia Sinica, Nankang, Taipei, Taiwan. [5]Department of Biology, Georgetown University, Washington, DC 20057, USA.

‡Authors for correspondence (hcc0609@tmu.edu.tw, ckshen@imb.sinica.edu.tw)

Received 5 June 2013; Accepted 8 May 2014

Journal of Cell Science (2014) 127, 3024–3038 doi:10.1242/jcs.136150

2011; Avendaño-Vázquez et al., 2012; Polymenidou et al., 2011). Despite the above studies, however, the overall picture of the degradation program of the different TDP protein species, i.e. the full-length TDP-43, and the TDP-35 and TDP-25 fragments, in normal cells remain unclear.

The roles of the cleavage of TDP-43 by caspase 3 and the resulting TDP-25 and TDP-35 fragments in TDP-43 proteinopathies have also been studied in cell culture. One common observation is that overexpression of the TDP-25 fragment in yeast or cultured mammalian cells results in insolubility of TDP-43 species, as assayed by western blotting of fractionated cell extracts, and the formation of cytoplasmic TDP-43-positive aggregates, as assayed by immunofluorescence staining (Furukawa et al., 2011; Igaz et al., 2009; Nonaka et al., 2009b; Saini and Chauhan, 2011; Zhang et al., 2009; Zhang et al., 2007). However, upon MG132 treatment, which causes accumulation of full-length TDP-43, owing to inhibition of UPS, and enhances the cleavage of the full-length TDP-43 to generate more TDP-35 and TDP-25 fragments, as the result of induction of caspase 3 (Kleinberger et al., 2010; Nonaka et al., 2009a), the amount of the cytosolic TDP-43-positive aggregates and/or insoluble TDP-43 species increases greatly. The above studies have suggested the importance of the TDP-35 and TDP-25 fragments and an elevated amount of the full-length TDP-43 in the formation of TDP-43-positive UBIs, a process in which pre-formed TDP-25 fibrils could act as the seed (Furukawa et al., 2011; Pesiridis et al., 2011) to trap the full-length TDP-43 *in vitro* in cultured cells and *in vivo* in diseased cells of patients with TDP-43 proteinopathies. However, data from other studies seem to indicate that the proteolytic processing of the full-length TDP-43 is not absolutely required for generation of the insoluble TDP-43, nor does the generation of insoluble TDP-43 species necessarily lead to the aggregate formation (Dormann et al., 2009; Kleinberger et al., 2010). For instance, exogenous expression of caspase-3-resistant mutant TDP-43 (D89A) in HeLa cells, which is present in the insoluble fraction, does not lead to formation of TDP-43 (D89A) aggregates in these cells (Dormann et al., 2009).

Thus, despite the progresses regarding the processes of degradation/metabolism of TDP-43 in normal and diseased cells, several important questions remain unanswered: (1) are degradation pathways other than UPS and macroautophagy, such as CMA, also involved in TDP-43 degradation; (2) what are the degradation pathway(s) of the endogenous truncated TDP-43 fragments; (3) what are the relative contributions of the different metabolic routes to the degradation of TDP-43 (endogenous or exogenous, full-length versus truncated TDP-35 and TDP-25 fragments) have not been determined; and (4) what is the exact role of the truncated TDP-43 fragments in the generation of insoluble TDP-43 species and/or formation of the TDP-43-positive aggregates, respectively. To address the above, we have carried out a comprehensive study of the pathways of the metabolism and mis-metabolism of TDP-43.

RESULTS

Metabolism of TDP-43 protein by the CMA-mediated lysosome degradation pathway

Several previous studies have shown that both the UPS and macroautophagy pathways are involved in TDP-43 protein degradation. However, whether other degradation pathways such as the CMA participate in TDP-43 degradation remained unclear. In the CMA pathway, substrate proteins bearing the KFERQ-like motif are recognized by heat shock protein Hsc70 (also known as HSPA8) and this substrate–chaperone complex is targeted to the lysosome membrane receptor LAMP-2A for further endocytosis and lysosomal degradation (Dice, 2007). We noticed that the RRM1 domain of TDP-43 contained the CMA-recognition motif sequence $Q^{134}VKKD^{138}$ (Fig. 1A), suggesting that TDP-43 might also be a CMA substrate. To investigate this possibility, we first determined whether TDP-43 interacted with Hsc70 by immunoprecipitation. Notably, the levels of ubiquitylated wild-type and mutant TDP-43 were both increased in the presence of HA–ubiquitin (supplementary material Fig. S1A). Furthermore, ubiquitylated wild-type TDP-43, but not mutant TDP-43 (QV/AA) in which the QVKKD sequence was mutated to AAKKD, interacted well with Hsc70 in the presence of the exogenous HA–ubiquitin (Fig. 1B; supplementary material Fig. S1B). This result suggests that an intact $Q^{134}VKKD^{138}$ motif is required for efficient Hsc70 interaction with ubiquitylated TDP-43 as well as translocation of TDP-43 to the lysosomal LAMP-2A.

We then analyzed whether TDP-43 could be degraded by CMA and whether the CMA-recognition motif was required for this process. For this, we compared the levels of wild-type and QV/AA-mutant TDP-43 proteins in transfected N2a cells with and without the lysosome inhibitor NH_4Cl (Cuervo et al., 2004; Mizushima et al., 2010; Tanida et al., 2005) (Fig. 1C). The levels of the TDP-35 and TDP-25 fragments of wild-type TDP-43 (Fig. 1C, compare lane 2 to lane 1; also see the histogram), but not the mutant TDP-43 (QV/AA) (Fig. 1C, compare lane 4 to lane 3; also see the histogram), were increased, albeit moderately, upon treatment with NH_4Cl. Because NH_4Cl is a general lysosomal inhibitor that represses CMA and macroautophagy, the participation of CMA in TDP-43 protein degradation was further assessed by RNA interference (RNAi)-mediated knockdown of the LAMP-2A receptor. There are three splice variants of LAMP-2, LAMP-2A, -2B and -2C, of which LAMP-2A is involved in CMA, whereas LAMP-2B and LAMP-2C function in macroautophagy (Massey et al., 2006; Cuervo and Dice, 2000; Hatem et al., 1995; Tanaka et al., 2000). In particular, it has been demonstrated that knockdown of LAMP-2A can just affect the ability of CMA substrate binding and uptake by the lysosomes rather than alter macroautophagy or lysosomal protease activity (Massey et al., 2006; Cuervo and Dice, 2000). In addition, knockdown of the LAMP-2B only affects the fusion of lysosome or autophagosome in macroautophagy, but not the CMA–lysosomal substrate metabolism pathway (Tanaka et al., 2000).

As shown in supplementary material Fig. S1C, only the LAMP-2A mRNA, but not those of LAMP-2B and LAMP-2C, was knocked down by the LAMP-2A siRNA oligonucleotide. Consistent with previous findings (Massey et al., 2006), conversion of LC3-I to LC3-II and induction of p62 were observed in the LAMP-2A-knockdown cells, indicating that macroautophagy was activated in the LAMP-2A-knockdown cells in compensation (supplementary material Fig. S1C). Importantly, as shown in Fig. 1D, when the level of the endogenous LAMP-2A was lowered by the specific siRNA oligonucleotide, the amounts of the endogenous TDP-35 and TDP-25 fragments, but not the full-length TDP-43, were modestly increased, even though macroautophagy was activated (supplementary material Fig. S1C). Taken together, the data of Fig. 1 and supplementary material Fig. S1C show that TDP-43 protein species, particularly the TDP-35 and TDP-25 fragments,

Journal of Cell Science (2014) 127, 3024–3038 doi:10.1242/jcs.136150

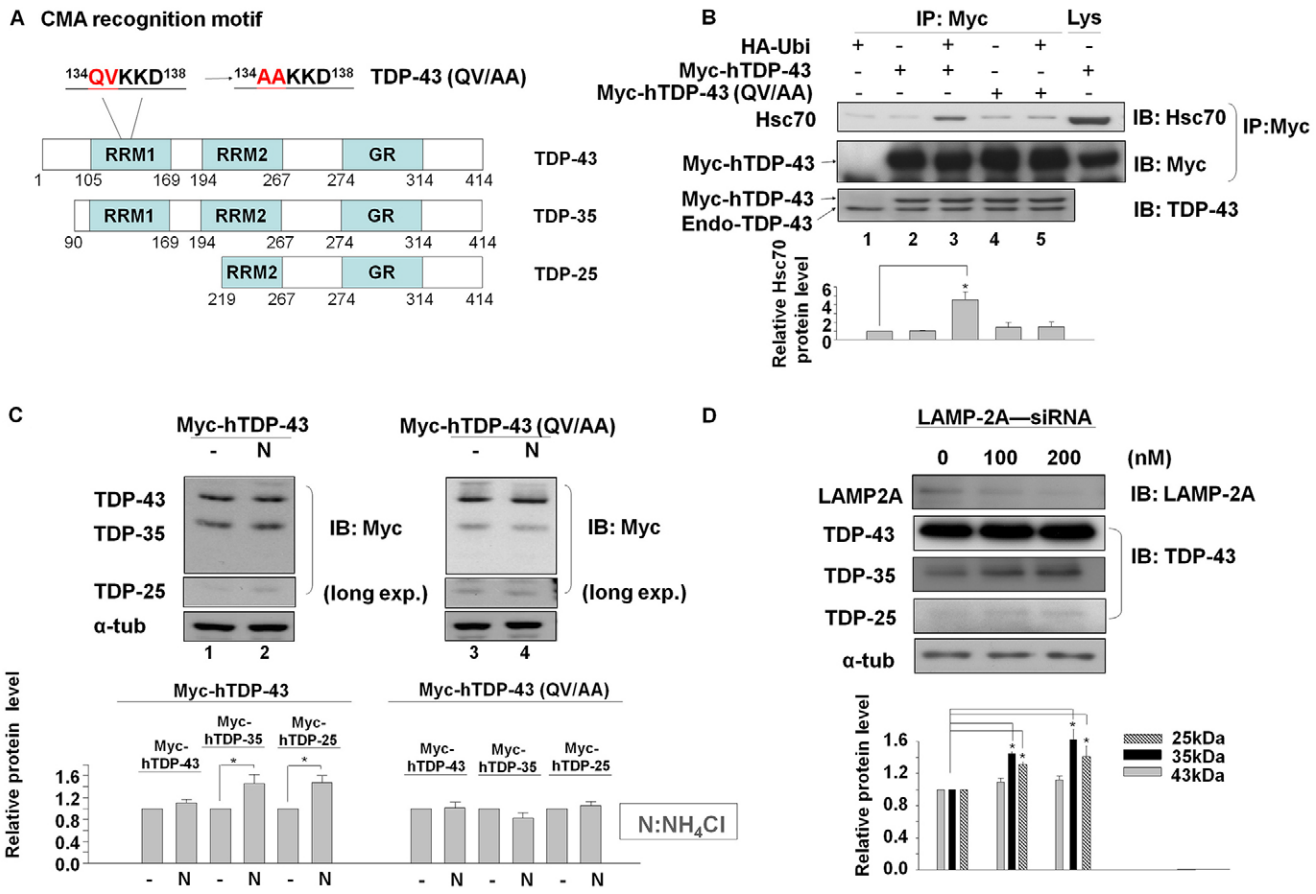

Fig. 1. Metabolism of TDP-43 proteins by the CMA-mediated lysosome degradation pathway. (A) The CMA-recognition motif in the RRM1 domain of hTDP-43. The CMA-recognition motifs in general consist of a glutamine residue (Q) flanked on either side by a basic amino acid (K or R), an acidic amino acid (D or E), a bulky hydrophobic amino acid (F, I, L or V) and a repeat of basic or bulky hydrophobic amino acid (Dice, 2007). Following this rule, a putative CMA-recognition motif ($Q^{134}VKKD^{138}$) was identified in the RRM1 region of human hTDP-43. Both the wild-type hTDP-43 and a mutant form of hTDP-43 (QV/AA) were studied in B and C below. (B) Western blotting shows the interaction between hTDP-43 or hTDP-43 (QV/AA) with Hsc70. 293T cells were transiently transfected with pMyc-hTDP-43 or pMyc-hTDP-43 (QV/AA) with or without pHA-Ub for 48 h, and then treated with NH_4Cl for 18 h. The cell lysates were immunoprecipitated (IP) with anti-Myc and then immunoblotted with anti-TDP-43 antibody (epitope, amino acids 1–260), anti-Hsc70 and anti-Myc, respectively. Endo-TDP-43, endogenous TDP-43. Lys, input lysate. (C) Effect of NH_4Cl on the levels of hTDP-43 species in transfected N2a cells. N2a cells were transiently transfected with pMyc-hTDP-43 or pMyc-hTDP-43 (QV/AA) for 48 h and then treated with 20 mM NH_4Cl for 18 h. The total cell lysates were extracted with the urea buffer and the levels of different wild-type Myc-hTDP-43 or mutant Myc-hTDP-43 (QV/AA) species were analyzed by western blotting with use of anti-Myc. (D) N2a cells were transiently transfected with control siRNA oligonucleotide or mouse LAMP-2A-specific siRNA oligonucleotides (100 nM or 200 nM) for 48 h, and the levels of the endogenous TDP-43, TDP-35 and TDP-25 fragments and LAMP-2A were examined by western blotting with use with anti-TDP-43 antibody (epitope, amino acids 1–260). Data are presented as mean±s.e.m. of three independent experiments. *$P<0.05$ by Student's *t*-test compared with the control.

can also be degraded through CMA in normal cells, although much more degradation was attributed to UPS (see below).

Relative contributions of UPS, macroautophagy and CMA to the degradation of endogenous and exogenously expressed TDP-43

Given that TDP-43 appeared to be processed and degraded by CMA in addition to by the UPS and macroautophagy (Fig. 1), it was of interest to obtain a comprehensive picture of the relative contributions of the three pathways of TDP-43 protein metabolism under normal cellular conditions. To this end, we first compared the levels of the exogenously expressed Myc-tagged human TDP-43 (hTDP-43) in transfected N2a cells upon treatment with the UPS inhibitor MG132, the macroautophagy inhibitor 3-methyladenine (3-MA), or NH_4Cl. Similar to previous studies (Bjørkøy et al., 2005; Kuusisto et al., 2001; Wong et al., 2008), in transfected or untransfected cells, the level of p62 was increased upon treatment with any one of these three inhibitors (supplementary material Fig. S1D, upper two panels). In addition, the level of LC3-II and/or the ratio of LC3-II:LC3-I was increased in cells treated with MG132 or NH_4Cl but not 3-MA (supplementary material Fig. S1D, middle 2 panels), as reported previously (Cheong et al., 2011; Hu et al., 2012; Iwata et al., 2005). Consistent with the literature (see the Introduction) and our data (Fig. 1), both the UPS and the autophagy, including macroautophagy and CMA, were responsible for the degradation of the exogenous Myc–hTDP-43 protein (Fig. 2A). However, only modest increases of the full-length Myc–hTDP-43 was observed upon treatment with any of the three inhibitors including NH_4Cl. By contrast, the accumulation of 35 kDa and 25 kDa Myc–hTDP-43 fragments was significantly higher, particularly in MG132-treated cells (Fig. 2A).

From the data of Fig. 2, in particular, the changes in the total amounts of the different TDP-43 species upon the use of these

Journal of Cell Science (2014) 127, 3024–3038 doi:10.1242/jcs.136150

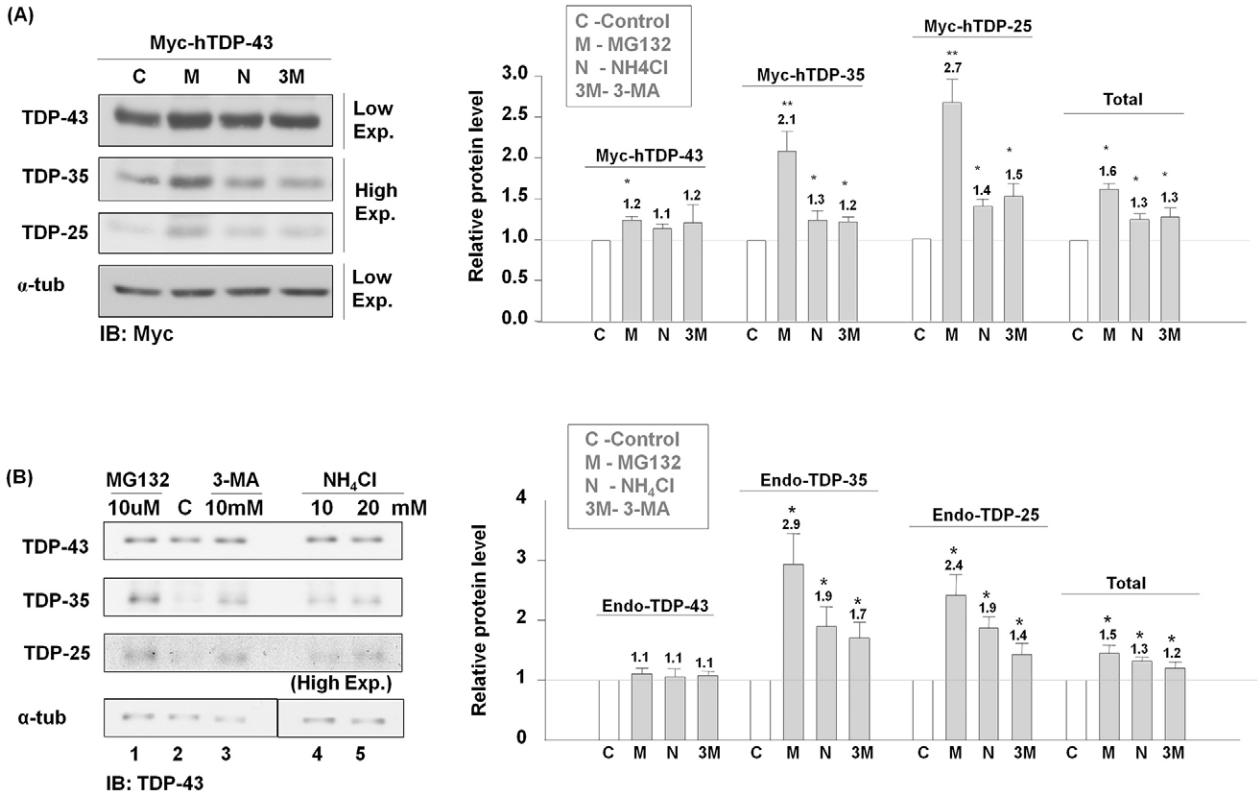

Fig. 2. Relative contributions of UPS, macroautophagy and CMA to the degradation of endogenous and exogenously expressed TDP-43. (A) N2a cells were transfected with pMyc-hTDP-43 for 48 h and then treated with different inhibitors: 20 mM of NH_4Cl (N), 10 mM 3-MA (3M) or 10 μM of MG132 (M) for 18 h. The total lysates were extracted with urea buffer and the protein levels of Myc-tagged hTDP-43 species were analyzed by western blotting with use of anti-Myc and anti-α-tubulin antibody. A quantification of the levels of total, full-length TDP-43, TDP-35 and TDP-25 fragments of Myc-tagged hTDP-43 in drug-treated cells in comparison to the untreated cells (control, C) is shown in the histogram on the right. The data are presented as mean±s.e.m. of three independent experiments. *$P<0.05$; **$P<0.01$ (Student's *t*-test compared with the control). (B) Untransfected N2a cells were treated with different inhibitors: NH_4Cl (10 and 20 mM), 3-MA (10 mM) or MG132 (10 μM) for 18 h. The total lysates were extracted with urea buffer and the levels of different TDP-43 species were analyzed by western blotting with use with anti-TDP-43 antibody (epitope, amino acids 1–260). A quantitative comparison is shown in the histogram on the right. Endo-TDP-43, endogenous TDP-43. The data are presented as mean±s.e.m. of three independent experiments. *$P<0.05$ (Student's *t*-test compared with the control). Please note that the backgrounds of lanes 1–3 and lane 4–5 on the bottom image panel of B have been adjusted to a similar level in the figure.

three inhibitors, we estimated that the contributions of the three pathways to the processing and degradation of the endogenous and exogenous TDP-43 proteins were in the order of UPS>CMA≥macroautophagy.

Cleavage of the full-length TDP-43 into TDP-35 and TDP-25 fragments is a necessary intermediate step in TDP-43 degradation

The greater accumulation of the endogenous TDP-25 and TDP-35 fragments than the full-length TDP-43 in LAMP-2A-knockdown cells (Fig. 1D) and in MG132-, 3-MA- or NH_4Cl-treated cells (Fig. 2B) suggests that truncated TDP-43 fragments are more prone to degradation through the UPS and autophagy pathways. In general, full-length TDP-43 can be degraded through two routes: either the full-length TDP-43 itself can be degraded directly, or the full-length TDP-43 can be first cleaved into truncated fragments and then degraded by the UPS and autophagy pathways. The data in Figs 1 and 2 indicate that cellular TDP-43 protein is preferentially degraded through the second route because the accumulation of the total TDP-43 protein, as the result of UPS, macroautophagy or CMA inhibition, was mainly due to the accumulation of the TDP-35 and TDP-25 fragments. Thus, cleavage of the full-length TDP-43 into TDP-35 and TDP-25 appears to be a necessary intermediate step for degradation of most of the cellular TDP-43 protein. To validate this result, we compared the half-life of the endogenous full-length TDP-43 protein in N2a cells treated with and without the caspase 3 inhibitor Z-VAD. The effects of MG132 and Z-VAD on the level of active caspase 3 were verified in supplementary material Fig. S1E, showing that enhanced cleavage of the pro-caspase 3 was observed in MG132-treated cells whereas Z-VAD treatment inhibited this enhancement. The data from cyclohexamide chase experiments showed that Z-VAD treatment increased the half-life of the TDP-43 protein from 31 h, a value similar to the findings of Pesiridis et al. (Pesiridis et al., 2011), to over 75 h (Fig. 3A).

We then transfected N2a cells with pMyc-hTDP-43 or pMyc-hTDP-43 (D89A), and measured the half-life of the full-length Myc–hTDP-43, caspase-cleavage-resistant Myc–hTDP-43 (D89A), and Myc–hTDP-35 and Myc–hTDP-25 fragments by the cycloheximide chase assay (Fig. 3B). The half-life of Myc–hTDP-43 and Myc–hTDP-43 (D89A) were also measured by [^{35}S]methionine pulse-chase assay (supplementary material Fig. S2A). Similar to the previous findings (Urushitani et al., 2010), the half-lives of the full-length Myc–hTDP-43 and the truncated Myc–hTDP-35 and Myc–hTDP-25 were ~16–18 h, ~10 h and ~7.6 h, respectively (Fig. 3B; supplementary material Fig. S2A).

Journal of Cell Science (2014) 127, 3024–3038 doi:10.1242/jcs.136150

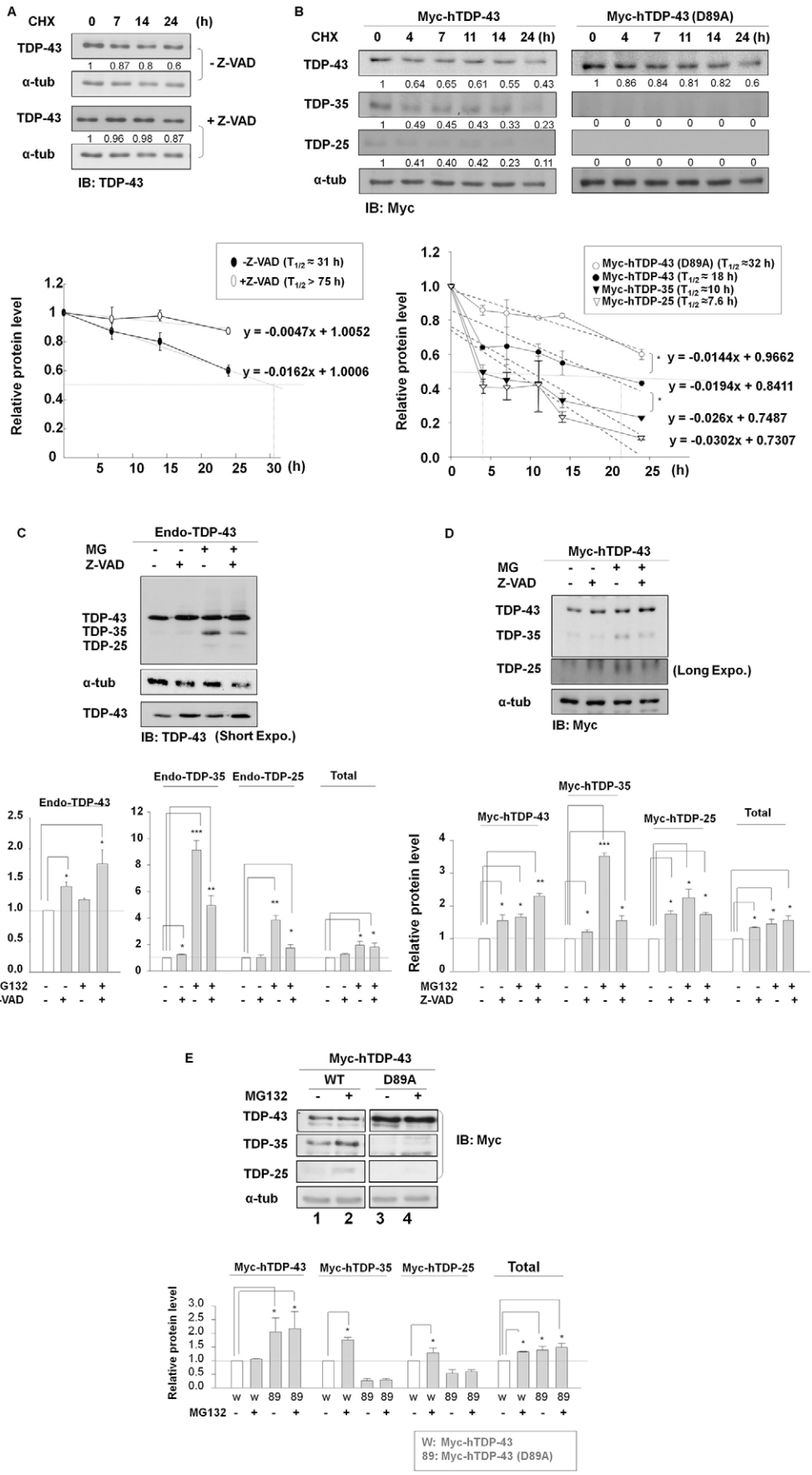

Fig. 3. See next page for legend.

Journal of Cell Science

Journal of Cell Science (2014) 127, 3024–3038 doi:10.1242/jcs.136150

Fig. 3. Cleavage of full-length TDP-43 into the TDP-35 and TDP-25 fragments as a necessary intermediate step of TDP-43 degradation. (A,B) Z-VAD effect on the half-life of endogenous TDP-43 proteins. N2a cells were treated with cycloheximide (CHX, 20 μg/ml) with or without the co-presence of the caspase inhibitor Z-VAD (50 μM). The total lysates were extracted with urea buffer and the levels of the endogenous TDP-43 at different time points of the treatment were analyzed by western blotting with use of anti-TDP-43 antibody (epitope, amino acids 1–260) (A). Effect of TDP-43 (D89A) mutation on the half-life of exogenous Myc-hTDP-43 protein. N2a cells were transfected with pMyc-hTDP-43 or pMyc-hTDP-43 (D89A) for 48 h, and then treated with cycloheximide (20 μg/ml) for different time periods. The total lysates were extracted with urea buffer and the protein levels of the full-length Myc–hTDP-43, Myc–hTDP-35 and Myc–hTDP-25 in pMyc-hTDP-43 and pMyc-hTDP-43 (D89A) transfected cells were analyzed by western blotting with use of anti-Myc antibody (B). The graphs below the blots in A and B show a quantification of the relative values at each time point, from which the half-lives of the proteins were estimated according to the equation of the regression lines as $y=ax+b$. (C) Effects of Z-VAD and/or MG132 on the levels of the different TDP-43 species. N2a cells were treated with MG132 (10 μM), Z-VAD (50 μM) or both for 18 h. The levels of TDP-43, TDP-35 and TDP-25 were then analyzed by western blotting with use of anti-TDP-43 antibody (epitope, amino acids 1–260). Endo-TDP-43, endogenous TDP-43. (D) Effects of Z-VAD and/or MG132 on the levels of exogenous Myc-hTDP-43. N2a cells were transfected with pMyc-hTDP-43 for 48 h and then treated with MG132 (10 μM) and/or Z-VAD (50 μM) for 18 h. The total lysates were extracted with urea buffer and the protein levels of the full-length Myc-hTDP-43 and its truncated Myc-hTDP-35 or -25 fragments were analyzed by western blotting with use of anti-Myc antibody. (E) Effect of D89A mutation on the accumulation of different TDP-43 species. N2a cells were transfected with pMyc-hTDP-43 or pMyc-hTDP-43 (D89A) for 48 h and then treated with 10 μM MG132 for 18 h. The total lysates were extracted with urea buffer and analyzed by western blotting with use of anti-Myc antibody. W, WT, wild-type TDP-43. In the histogram, the data are presented as mean±s.e.m. of three independent experiments. ***$P<0.005$; **$P<0.01$; *$P<0.05$ (Student's *t*-test compared with the control). Please note that the left two lanes of gel piece and the right two lanes of gel piece in E were separated by other lanes (not shown) on the same gel, but their images are spliced together in the figure.

Interestingly, although the mRNA levels of Myc–hTDP-43 and Myc–hTDP-43 (D89A) in the transfected N2a cells were similar (supplementary material Fig. S2B), the caspase-3-resistant, full-length Myc–hTDP-43 (D89A) had a significantly longer half-life than the wild-type full-length Myc–hTDP-43 (Fig. 3B; supplementary material Fig. S2A). The difference of the half-lives of Myc–hTDP-43 (D89A) in Fig. 3B and supplementary material Fig. S2A, as measured by the two assays, likely results from the different experimental procedures used. This result further suggested that majority of TDP-43 is degraded through UPS or the autophagy pathways after the caspase-cleavage step, and TDP-43 resistant to the cleavage into TDP-25 and TDP-35 fragments has a longer half-life.

To further assess the importance of TDP-25 and TDP-35 fragments as the intermediates in TDP-43 degradation, we compared the accumulation patterns of the full-length TDP-43 in N2a cells upon treatment with MG132 and/or Z-VAD. We found that the level of the full-length endogenous (Fig. 3C) or exogenous TDP-43 (Fig. 3D) in cells treated with Z-VAD was higher (1.5- or 2-fold) than that without Z-VAD treatment, regardless of the presence of MG132. We also compared the accumulation patterns of the exogenous Myc–hTDP-43 and Myc–hTDP-43 (D89A) with or without treatment with MG132. As shown by western blotting, the D89A mutation indeed led to the disappearance of the TDP-35 and TDP-25 fragments (Fig. 3E, compare lanes 3 and 4 to lanes 1 and 2, respectively). Furthermore, the level of Myc–hTDP-43 (D89A) was ~2-fold higher than that of Myc–hTDP-43 (Fig. 3E, compare lane 3 to lane 1), and this higher level of Myc–hTDP-43 (D89A) persisted in the presence of MG132 (Fig. 3E, compare lane 4 to lane 3). This correlated well with the data presented in Fig. 2A, in which MG132 treatment resulted in only a modest increase of the full-length Myc-hTDP-43 but a 2-fold increase of the TDP-35 and TDP-25 fragments (Fig. 3E, compare lane 2 to 1). This suggests that the D89A mutation conferring resistance of TDP-43 to the cleavage by caspase 3 indeed prolonged the half-life of the full-length TDP-43 protein. The data in Fig. 3 were thus consistent with the hypothesis that cleavage of TDP-43 by caspase 3 to generate the 35 kDa and 25 kDa species is an important intermediate step for the eventual degradation of TDP-43 protein.

Contributions of UPS, macroautophagy and CMA to the formation of TDP-43-positive aggregates

Given that CMA is also involved in TDP-43 degradation (Fig. 1), we tested the effect of CMA inhibition on the formation of TDP-43-positive cytosolic aggregates in comparison to that induced by UPS and macroautophagy inhibition. Immunofluorescence staining analysis demonstrated that the cytosolic TDP-43 was mostly diffuse upon MG132 treatment, and no TDP-43-positive aggregation could be observed in NH_4Cl- or 3MA-treated cells (Fig. 4A, upper histogram). Notably, C-terminal fragments (CTFs) containing RRM2, as generated from *de novo* cleavage of nuclear TDP-43, are transported to the cytoplasm and efficiently cleared, indicating that cleavage alone is not sufficient to initiate the CTF aggregation (Pesiridis et al., 2011). However, a significant fraction (~30%) of pMyc-hTDP-43-transfected N2a cells contained cytosolic Myc–hTDP-43-positive aggregates upon MG132 treatment (Fig. 4B), suggesting that an excess of TDP-43 is required for the aggregate formation. Importantly, inhibition of CMA and macroautophagy by using NH_4Cl, or inhibition of macroautophagy by 3-MA, induced ~10% of the transfected cells to form cytosolic Myc–hTDP-43-positive aggregates (Fig. 4B). Therefore, blockage of the degradation (CMA and macroautophagy) of TDP-43 by NH_4Cl indeed can also induce the formation of cytosolic TDP-43-positive aggregates if sufficiently high levels of TDP-43 are present. This result was supported by the analysis of aggregate formation in transfected N2a cells expressing wild-type Myc–hTDP-43 or the Myc–hTDP-43 (QV/AA) mutant (Fig. 4C), in which the percentage of transfected cells containing the TDP-43 (QV/AA) mutant that showed cytoplasmic aggregates (9.8%) was higher than that of cells expressing the wild-type Myc–hTDP-43 (5.1%). The above results further support the hypothesis that TDP-43 protein is degraded in part through the CMA pathway as already shown in Figs 1 and 2. More importantly, the data of Fig. 4 demonstrates that blockage of the degradation of TDP-43 by CMA, with either use of NH_4Cl or by mutagenesis of the Hsc70 recognition site, also increases the extent of TDP-43-positive aggregate formation in transfected N2a cells containing an excess of the TDP-43 protein. These TDP-43-positive aggregates did not co-stain with the stress granule marker, TIA1 or HuR (supplementary material Fig. S3), indicating they were not stress granules.

Requirement of a threshold level of TDP-25 fragment for formation of the cytosolic TDP-43-positive aggregates

As mentioned in the Introduction, several DNA transfection studies in cell culture have shown the importance of the C-terminal 25 kDa fragment in the formation of the TDP-43-positive inclusions, but others using caspase 3 inhibitor or caspase 3-resistant TDP-43 seemed to suggest that proteolytic cleavage of

Journal of Cell Science (2014) 127, 3024–3038 doi:10.1242/jcs.136150

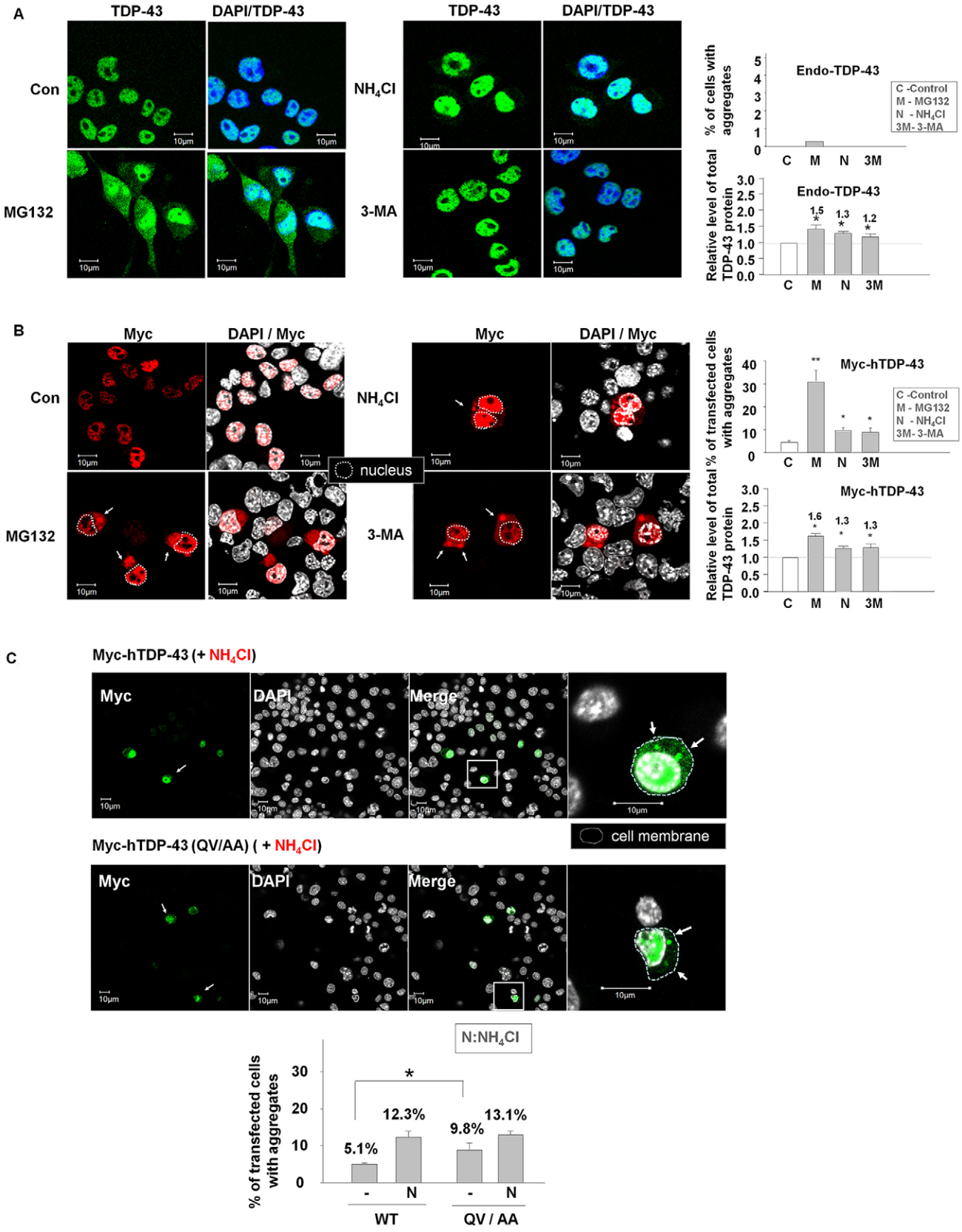

Fig. 4. See next page for legend.

Journal of Cell Science (2014) 127, 3024–3038 doi:10.1242/jcs.136150

Fig. 4. Contributions of UPS, macroautophagy and CMA to the formation of TDP-43-positive aggregates. (A) Immunofluorescence staining of N2a cells treated with different inhibitors with use of anti-TDP-43 antibody (epitope, amino acids 1–260) (green) and DAPI (blue). The histogram in Fig. 2B showing the relative levels of the total endogenous TDP-43 protein is duplicated here for comparison to the histogram showing of the percentage of cells with TDP-43-positive aggregates. Endo-TDP-43, endogenous TDP-43. (B) Immunofluorescence staining of N2a cells transfected with pMyc-hTDP-43 for 48 h and treated with 10 μM MG132, 20 mM NH_4Cl or 10 mM 3-MA for 18 h. The cells were stained with anti-Myc (red) and DAPI (white). The bar histogram in Fig. 2A showing the relative levels of the total Myc-tagged hTDP-43 species is duplicated here for comparison. (C) Effect of QV/AA mutation on the formation of Myc–hTDP-43-positive aggregates. N2a cells were transiently transfected with pMyc-hTDP-43 (WT) or the pMyc-hTDP-43 (QV/AA) mutant for 48 h, treated with 20 mM NH_4Cl for 18 h, and then immunofluorescence stained with anti-Myc and DAPI. Data are presented as mean±s.e.m. of three independent experiments $*P<0.05$; $**P<0.01$ (Student's *t*-test compared with the control).

the full-length TDP-43 to generate the TDP-25 and TDP-35 fragments was not required for the insoluble TDP-43 formation or aggregate formation (Dormann et al., 2009; Kleinberger et al., 2010). To further clarify the role of the C-terminal TDP-43 fragments in the formation of the insoluble TDP-43 species and/or the TDP-43-positive aggregates, we transfected N2a cells with pMyc-hTDP-43 or pMyc-hTDP-43 (D89A) and analyzed the amount of the insoluble full-length TDP-43 and the 25 kDa and 35 kDa fragments in the urea-soluble fraction, and the formation of cytosolic TDP-43-positive aggregates (Fig. 5). As seen in Fig. 5A, MG132 treatment of transfected cells with overexpressed Myc–hTDP-43 or Myc–hTDP-43 (D89A) resulted in the accumulation of insoluble TDP-43 species in the urea fraction, including the 25 kDa and the 35 kDa fragments, derived from both the endogenous and exogenous TDP-43 (Fig. 5A, compare lanes 2 and 4 to 1 and 3, respectively). Notably, the full-length protein level of the insoluble Myc–hTDP-43 (D89A) in untreated cells was as high as that of Myc–hTDP-43 or Myc–hTDP-43 (D89A) in MG132-treated cells (Fig. 5A, compare lane 3 to lanes 2 and 4). This data was consistent with the scenario that cleavage of the wild-type TDP-43 by caspase 3 to generate the 35 kDa and 25 kDa species was an intermediate step in the cellular degradation of TDP-43, as already observed in Fig. 3. By contrast, the extent of formation of the cytoplasmic Myc–hTDP-43-positive aggregates in the cells transfected with pMyc-hTDP-43 (D89A) N2a cells without MG132 treatment was very low (less than 5%) (Fig. 5B, the third row of panels and the histogram), whereas the aggregate percentage in cells transfected with pMyc-hTDP-43 (D89A) upon MG132 treatment was comparable to that in MG132-treated Myc–hTDP-43-expressing cells (Fig. 5B, the second and fourth rows of panels and the histogram). These data show that the accumulation of insoluble TDP-43 in the urea fraction (Fig. 5A) and the formation of cytosolic TDP-43-positive aggregates (Fig. 5B) are not coupled. We infer that a minimum amount of the 25 kDa and 35 kDa fragments generated by the MG132-induced caspase-3 cleavage of the endogenous TDP-43 in N2a cells transfected with either pMyc-hTDP-43 and pMyc-hTDP-43(D89A) (Fig. 5A, lanes 2 and 4) is required as the seed for the aggregate formation by the full-length insoluble TDP-43 (Fig. 5B).

To test the above idea, we first carried out DNA transfection of N2a cells with different amounts of the plasmid pMyc-hTDP-25 expressing the Myc-tagged hTDP-25 fragment. As exemplified by the western blotting in supplementary material Fig. S4A, transfection of 3×10^5 N2a cells with 0.25 μg pMyc-hTDP-25 resulted in the expression of approximately similar molar concentration of Myc–hTDP-25 to that of the MG132-induced truncated endogenous TDP-25 fragment in N2a cells (supplementary material Fig. S4A, compare lanes 1 and 2). Therefore, we then co-transfected 3×10^5 N2a cells with 0.25 μg of pMyc-hTDP-25 together with either 2 μg pGFP-hTDP-43 or pGFP-hTDP-43 (D89A). The presence of 0.25 μg pMyc-hTDP-25, but not 0.1 μg pMyc-hTDP-25 or 0.25 μg pMyc vector, led to the formation of GFP–hTDP-43-positive or GFP–hTDP-43-(D89A)-positive aggregates in 25% of both sets of the co-transfected cells (Fig. 6B, compare bars 3 and 6 to bars 1, 2, 4 and 5), suggesting that formation of the TDP-43-positive aggregates was due to the presence of TDP-25 fragments as the seed rather than a stress of DNA transfection. Notably, we also co-expressed full-length TDP-43 with TDP-35 from 0.25 μg p-Myc-hTDP-35 because it was reported previously that TDP-35 could also cause aggregate formation (Che et al., 2011; Johnson et al., 2008; Zhang et al., 2009). However, the percentage (less than 15%) of these transfected cells that contained the aggregate was lower than that of cells co-expressing TDP-25 and TDP-43 (supplementary material Fig. S4C), consistent with the scenario that TDP-35 is an intermediate species for generation of the TDP-25 seed.

Following the above, we first estimated the absolute quantity of MG132-induced TDP-25 fragments in N2a cells under the conditions we used in Figs 5 and 6 (see Materials and Methods for more details), to determine the minimum content of TDP-25 that could serve as the seed for aggregate formation of excess full-length TDP-43. We carried out western blotting of an extract of MG132-treated N2a cells side by side with purified TDP-18 (amino acids 252–414), using an anti-TDP-43 antibody recognizing the C-terminal region of TDP-43 (amino acids 350–414) (supplementary material Fig. S4B). The band intensity of TDP-25 from 3×10^4 MG132-treated N2a cells (supplementary material Fig. S4B, lane 1) was similar to that of 20 ng of the purified TDP-18 (supplementary material Fig. S4B, lane 2), which corresponded to 1.1 pmole. Thus, the absolute amount of the 'seeding' TDP-25 fragment in MG132-treated cells would be $1.1/3\times10^4=3.6\times10^{-5}$ pmole/cell.

We calculated the absolute amount of the total full-length TDP-43 that was sufficient to form the aggregates in the presence of the TDP-25 seed from the data shown in supplementary material Fig. S4B and Fig. 5. Comparison of the intensities of the different bands in lane 1 of supplementary material Fig. S4B indicated that the intensity of the endogenous TDP-43 in MG132-treated cells was nine times that of the endogenous TDP-25. This corresponded to $3.6\times10^{-5}\times9=3.2\times10^{-4}$ pmole/cell. Furthermore, the band intensities of Myc–hTDP-43 and the endogenous full-length TDP-43 in extracts of N2a cells transfected with pMyc-hTDP-43 and treated with MG132 were in the ratio of 1:1.7 (Fig. 5A). Thus, the absolute total amount of the full-length TDP-43 including the exogenous Myc-hTDP-43 and endogenous TDP-43 in the N2a cells transfected with pMyc-hTDP-43 and treated with MG132 (Fig. 5) would be $3.2\times10^{-4}\times(1+1.7)=8.6\times10^{-4}$ pmole/cell. Thus, on the average, $\sim3.6\times10^{-5}$ pmole/cell of the TDP-25 protein fragment is necessary and sufficient to function as the seed for effective formation of TDP-43-positive aggregates, if there is also a sufficiently elevated level of the full-length TDP-43 accumulated in the cells (see Discussion).

DISCUSSION

In this study, we have carried out a comprehensive study of the metabolism and mis-metabolism of TDP-43. We show that the internal cleavage of TDP-43 by caspase 3 to generate the TDP-35

Journal of Cell Science (2014) 127, 3024–3038 doi:10.1242/jcs.136150

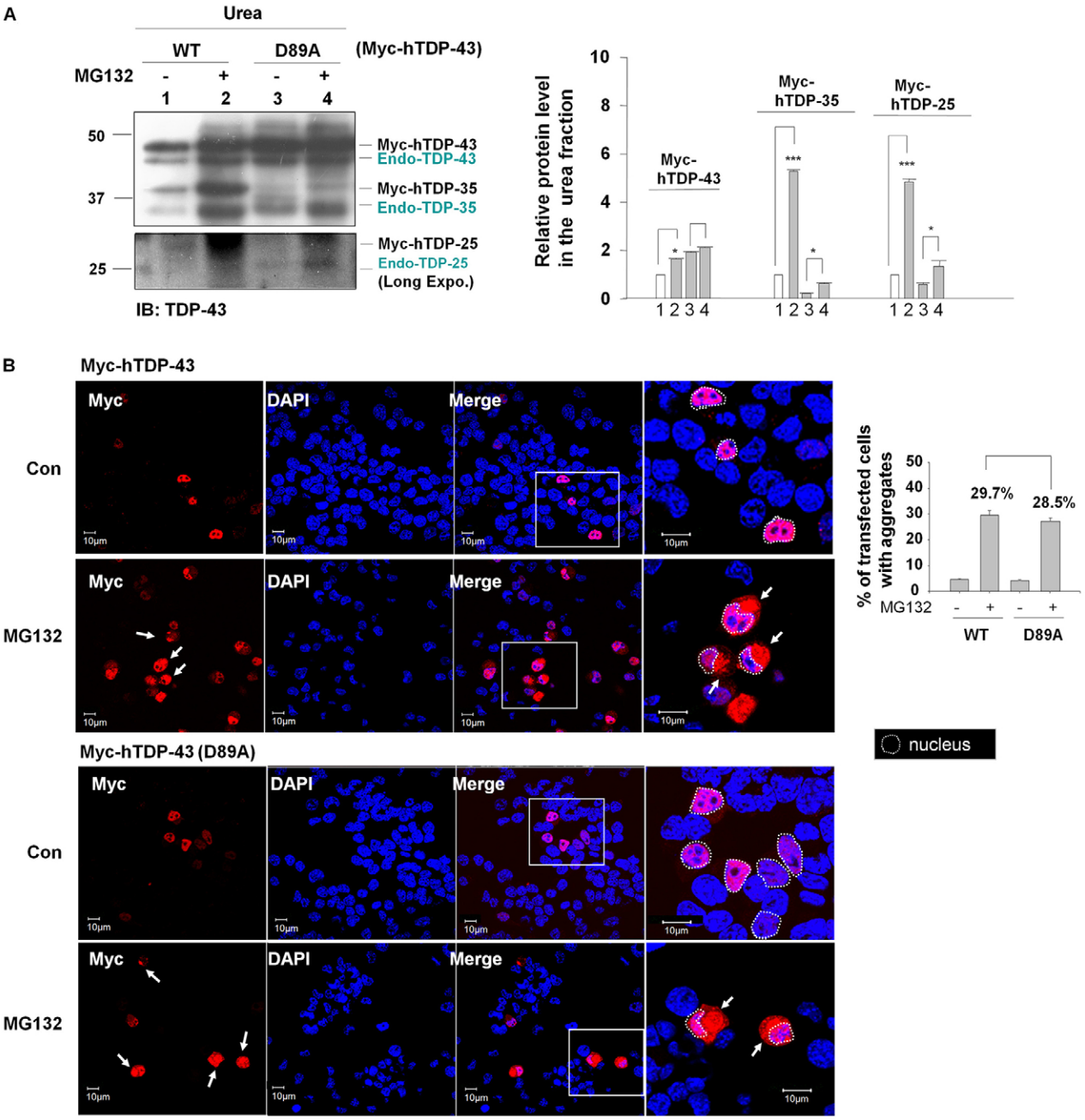

Fig. 5. Insolubilities and aggregate formation of Myc–hTDP-43 and Myc–hTDP-43 (D89A) in transfected N2a cells. (A) Relative insolubilities of Myc–hTDP-43 (WT) and Myc–hTDP-43 (D89A) protein species. N2a cells transfected with pMyc-hTDP-43 or pMyc-hTDP-43 (D89A) were treated with 10 μM MG132 for 18 h, and then the total cell extracts were separated into RIPA- and urea-soluble fractions as described in the Materials and Methods. The banding patterns of the different TDP-43 protein species in the urea-soluble fractions were analyzed by western blotting with use of anti-TDP-43 antibody (epitope, amino acids 350–414). (B) Immunofluorescence images of N2a cells stained with anti-Myc antibody (red) with or without (Con) MG132 treatment. The percentage of cells with the red anti-Myc antibody signals that contained cytosolic aggregates were calculated and presented in the histogram. The data are presented as mean±s.e.m. of three independent experiments. *$P<0.05$; **$P<0.01$; ***$P<0.005$ (Student's *t*-test).

and TDP-25 fragments is a major intermediate step in the eventual degradation of the TDP-43 protein under normal conditions by different cellular pathways including UPS, macroautophagy and CMA. In addition, we clarify the seemingly confusing uncertainty regarding the requirement of the proteolytic cleavage of TDP-43 for the generation of insoluble TDP-43 species and/or the formation of cytosolic TDP-43-positive aggregates or inclusions. Equally important, we determine the minimum amount of the TDP-25 fragment as a seed for the formation of aggregates in the presence of a threshold cellular level of the full-length TDP-43. Some of the experiments have been conducted with use of other cell lines, human 293T cells or NSC-34 cells, and the data and conclusions obtained were similar (Fig. 1B; supplementary material Figs S1A,B; and data not shown). A model outlining these points of TDP-43 metabolism and mis-metabolism in relation to TDP-43 proteinopathies is shown in Fig. 7.

Journal of Cell Science (2014) 127, 3024–3038 doi:10.1242/jcs.136150

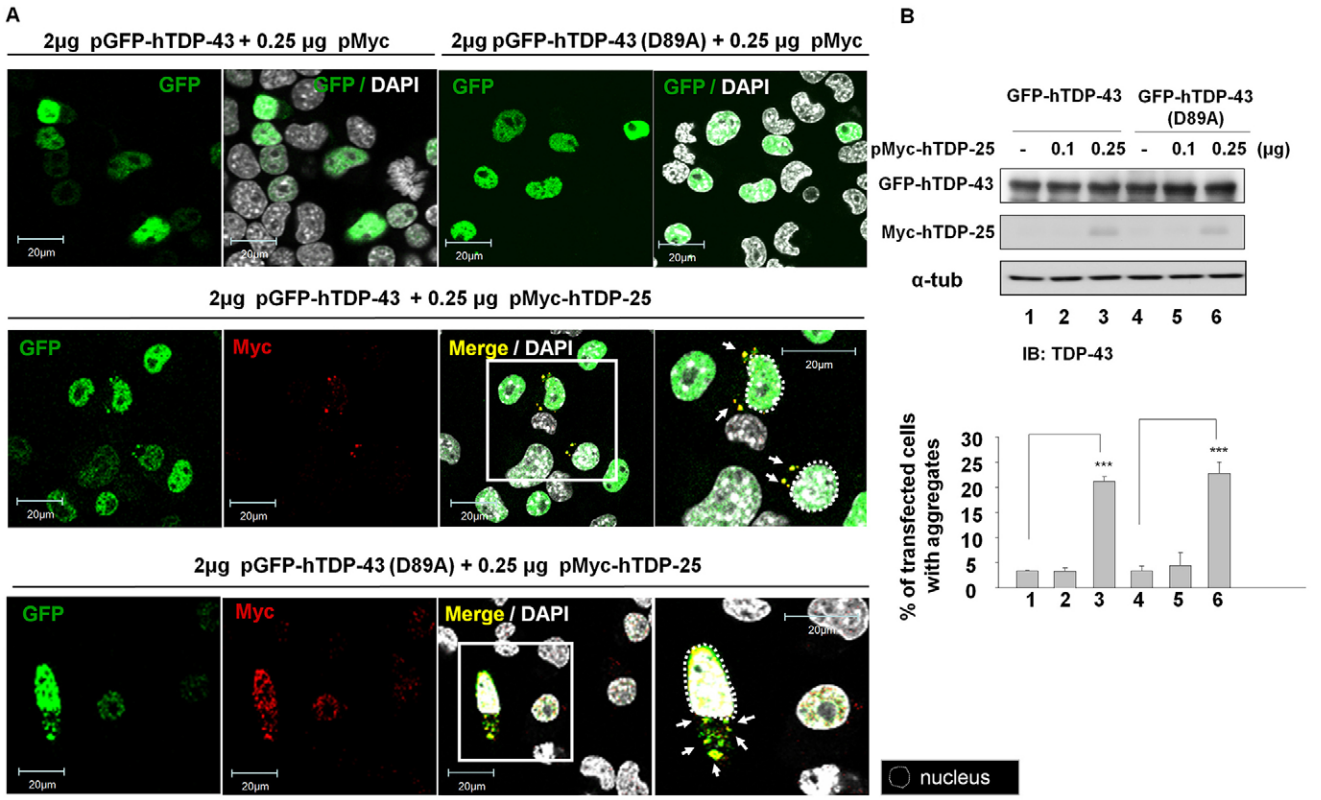

Fig. 6. Requirement of a threshold level of the 25 kDa fragment for formation of cytosolic TDP-43-positive aggregates. 3×10^5 N2a cells were transfected with 2 μg pGFP-hTDP-43 or pGFP-hTDP-43 (D89A), without (top row of panels in A) or with co-transfection (lower two rows of panels in A) of 0.1 μg or 0.25 μg of pMyc-hTDP-25 for 48 h. (A) Immunofluorescence patterns of the transfected N2a cells with use of anti-Myc (red) and DAPI (white). (B) Top panels, representative western blotting patterns of GFP–hTDP-43 and GFP–hTDP-43 (D89A) (upper panel), and Myc–TDP-25 (lower panel) of the transfected cells. Total lysates of transfected N2a cells were prepared by urea buffer extraction and then analyzed by western blotting with use of anti-TDP-43 antibody (epitope, amino acids 1–260). Bottom histogram, statistical analysis of the percentage of transfected cells with aggregates. The data are presented as mean±s.e.m. of at least two independent experiments. ***$P<0.005$ (Student's *t*-test).

Several studies have demonstrated the roles of UPS and macroautophagy degradation in the metabolism of TDP-43. Here, we show for the first time that the lysosome-dependent CMA participates in the degradation of TDP-43 in normal cells (Fig. 1; supplementary material Fig. S1). In particular, the CMA-recognition motif-like sequence in the RRM1 domain of TDP-43 facilitates the interaction between ubiquitylated TDP-43 and Hsc70 (Fig. 1B; supplementary material Fig. S1B). The data of Fig. 1B and supplementary material Fig. S1B provide the first evidence that the ubiquitylation is required for interaction of a CMA substrate with Hsc70. Perhaps this gives a general mechanism whereby certain ubiquitylated UPS substrate proteins also shuttle to the lysosomes for CMA degradation. Furthermore, mutation of CMA-recognition motif (Fig. 1C) and LAMP-2A-knockdown (Fig. 1D) lead to the accumulation of TDP-43 protein, suggesting that the N-terminal domain containing the CMA-recognition motif is indeed important for Hsc70-mediated TDP-43 protein translocation into the lysosome. Although the truncated 25 kDa and 35 kDa fragments of TDP-43 do not contain any CMA-recognition-motif-like sequence, nor do they bind Hsc70 (data not shown), our results show that it is mainly these fragments, and not the full-length TDP-43, that accumulates when CMA is inhibited (Figs 1 and 2). The lysosomes contain a large variety of hydrolytic enzymes, including cathepsins (cysteine proteases), aspartate proteases and one zinc protease, that degrade proteins and other substances taken in by endocytosis (McGrath, 1999; Nomura et al., 1999). Interestingly, in addition to caspase 3, other lysosomal proteases such as calpain and cathepsins might also mediate the cleavage of TDP-43 protein (Kanazawa et al., 2011; Yamashita et al., 2012). Furthermore, the caspase inhibitor Z-VAD that we have used in this study (Fig. 3A,C,D) also inhibit the lysosomal enzyme cathepsin B (Schotte et al., 1999). In addition, mass spectrometric analysis of extracts from brains from patients with FTLD-TDP (Nonaka et al., 2009b) suggests that caspase 3 might not be the only enzyme responsible for TDP-43 cleavage. Hence, we infer that in the CMA-mediated degradation pathway, once TDP-43 is transported to the lysosomes by Hsc70 and into the lysosomes by endocytosis, it would be cleaved into the TDP-25 and TDP-35 fragments by the lysosomal cathepsin B and then be subject to further degradation by the lysosomal proteases. Accordingly, in NH_4Cl-treated or LAMP-2A-knockdown cells (Figs 1, 2; supplementary material Fig. S1), the CMA proteolytic processing, such as endocytosis, cleavage and degradation, of TDP-43 inside the lysosomes would be slowed down or inhibited, and the full-length TDP-43 would be preferentially cleaved in the cytosol by active caspase 3. Therefore, inhibition of TDP-43 degradation by CMA would result in the accumulation of the truncated TDP-43 fragments, but not much of the full-length TDP-43.

Related to the above, several other neuropathological proteins, such as the Parkinson-disease-related α-synuclein and Alzheimer-disease-related RCAN1, have also been found to be degraded

Journal of Cell Science (2014) 127, 3024–3038 doi:10.1242/jcs.136150

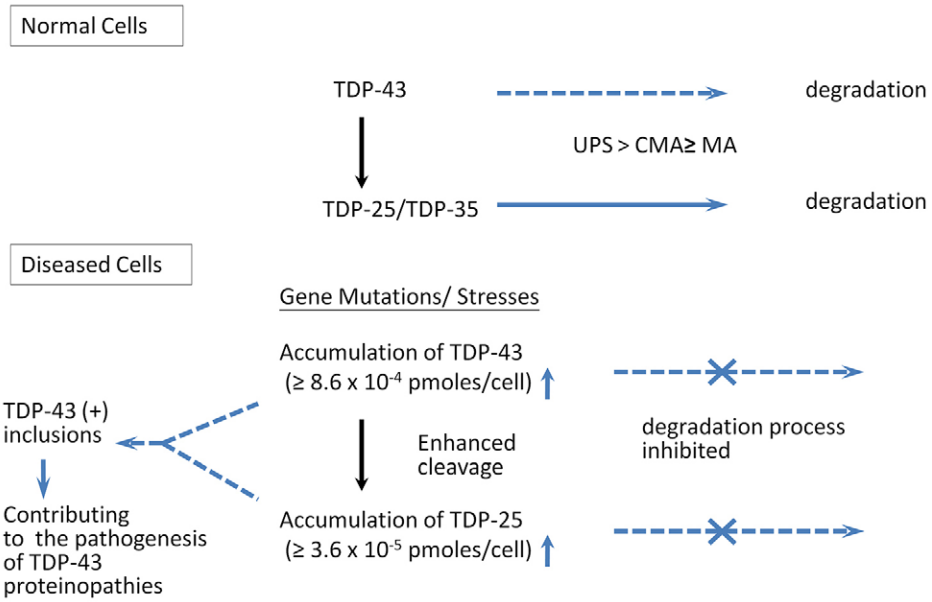

Fig. 7. A comprehensive model of the metabolism and mis-metabolism of TDP-43. A model of the metabolism of the TDP-43 protein in normal cells and its mis-metabolism in the diseased cells, leading to the formation of TDP-43-positive aggregates, is shown. Under normal conditions, proteolytic cleavage, by caspase 3 (Zhang et al., 2007), is a necessary intermediate step for degradation of the majority of TDP-43 protein through the processing of the TDP-25 and TDP-35 fragments by UPS, macroautophagy and CMA. In TDP-43 proteinopathies as caused by gene mutations or environmental stresses (Bigio, 2011; Boillée et al., 2006; Braun et al., 2011; Chen-Plotkin et al., 2008; Kwong et al., 2007; Mishra et al., 2007; Neumann, 2009), the degradation of the different TDP-43 species is somehow inhibited. The proteolytic cleavage of TDP-43 into TDP-25 and TDP-35 is also enhanced in the diseased cells (Arai et al., 2006; Kabashi et al., 2008; Neumann et al., 2006; Sreedharan et al., 2008). The accumulations of TDP-43 and TDP-25, the latter of which serves as the seed (Furukawa et al., 2011; Pesiridis et al., 2011), would lead to the formation of the cytosolic TDP-43-positive aggregates. From the data of this study, it is estimated that $\sim 8.6\times10^{-4}$ pmole/cell of TDP-43 and 3.6×10^{-5} pmole/cell of the TDP-25 fragment would be sufficient to lead to the formation the cytosolic TDP-43-positive aggregates.

through the CMA pathway (Cuervo et al., 2004; Liu et al., 2009). In those studies, dysfunction of CMA leads to the accumulation of the aberrant disease proteins, suggesting that impaired CMA might lead to toxic gain-of-function and the consequent protein aggregation in the brains of Parkinson and Alzheimer disease patients. Notably, two groups have analyzed the gene expression patterns in the frontal cortex samples of FTLD-TDP patients by microarray profiling, and found that the expression of LAMP-2A is upregulated whereas a number of UPS-related genes are downregulated (Chen-Plotkin et al., 2008; Mishra et al., 2007). We speculate that in TDP-43 proteinopathies, impairment of the UPS might be compensated for by upregulation of the CMA–lysosome system. Thus, CMA plays an important role in TDP-43 degradation in normal cells, and it might be induced in diseased cells to help clean the mis-metabolized TDP-43 protein species and even the TDP-43-positive aggregates.

Our data also provide strong support for the hypothesis that cleavage of the full-length TDP-43 into the truncated TDP-35 and TDP-25 fragments is a necessary intermediate step for degradation of most of the TDP-43 protein in the normal cells. As shown in Figs 2 and 3, the TDP-43 species accumulated in cells treated with different inhibitors are mainly the TDP-35 and TDP-25 fragments but not full-length TDP-43. It should be noted that there are negative-feedback mechanism(s) for TDP-43 to autoregulate its protein level (Ayala et al., 2011; Avendaño-Vázquez et al., 2012; Polymenidou et al., 2011). Thus, the levels of the full-length TDP-43 and the 25 kDa and 35 kDa fragments would be higher without this autoregulatory scheme. Several papers have concluded that exogenous truncated TDP-43 fragments are more prone to degradation by UPS than the exogenous full-length TDP-43 protein (Caccamo et al., 2009; Pesiridis et al., 2011; Wang et al., 2010). However, alternative explanations could not previously be excluded. For example, overexpression of the truncated TDP fragments, as alien misfolded or mutant proteins, is toxic and could force the cells to speed up the clearance of the exogenous TDP-43 fragment(s) by UPS and/or autophagy. Therefore, higher accumulation of the exogenous truncated TDP fragment(s) than the endogenous full-length TDP-43 would be observed when the UPS or autophagy degradation pathways are inhibited (Caccamo et al., 2009; Wang et al., 2010). In addition, either UPS inhibition or overexpression of the truncated TDP-43 fragments could result in increased level of active caspase 3 (Suzuki et al., 2011; Zhang et al., 2009), thus leading to increased proteolytic cleavage of the full-length TDP-43 to generate more TDP-35 and TDP-25 fragments (Rutherford et al., 2008). In order to exclude the above mentioned side-effects due to overexpression of the truncated TDP-25 fragment or MG132 induction, we have carried out cyclohexamide-chase experiments and found that degradation of the endogenous full-length TDP-43 becomes slower in the presence of the caspase 3 inhibitor Z-VAD (Fig. 3A). In addition, the stability of the full-length Myc–hTDP-43(D89A) mutant, which is resistant to caspase 3 cleavage, is also higher than the full-length wild-type Myc–hTDP-43 in transfected N2a cells (Fig. 3B; supplementary material Fig. S2A). The data of Figs 2 and 3 together demonstrate that cleavage of the full-length TDP-43 into the TDP-35 and TDP-25 fragments of shorter half-life is indeed an intermediate step for the degradation of a majority of the cellular TDP-43 protein. The different degradation rates between the full-length TDP-43 and its truncated fragments (TDP-25 and TDP-35) might result from their different level of post-translational modifications. Notably, the truncated TDP-43 fragments have been reported to

Journal of Cell Science (2014) 127, 3024–3038 doi:10.1242/jcs.136150

have a higher level of ubiquitylation than the full-length TDP-43 (Wang et al., 2010) and thus could be more prone to degradation by UPS. The requirement for generation of an intermediate for effective degradation or metabolism of cellular proteins has been documented in the literature, for example, for the Alzheimer protein APP (De Strooper et al., 2010), the transcription factor TWIST (Demontis et al., 2006) and PEST-motif-containing proteins (Belizario et al., 2008). Thus, internal peptide cleavage coupled with ubiquitylation for degradation by UPS and/or autophagy appears to be a general scheme for regulation of the homeostasis of a category of proteins. In the case of TDP-43, mis-regulation of this scheme likely would lead to the formation of TDP-43-positive UBIs or aggregates in diseased cells with TDP-43 proteinopathies.

In this study, we have estimated the threshold level of TDP-25 fragment that would lead to the formation of TDP-43-positive aggregates in the presence of elevated level of total TDP-43 (Fig. 6; supplementary material Fig. S4A,B). This is of particular interest because TDP-25 has been shown to be able to function as the seed for TDP-43-positive aggregate formation (Furukawa et al., 2011; Pesiridis et al., 2011), but the threshold level of the endogenous TDP-25 'seed' for co-aggregation with the full-length TDP-43 in cells had not been determined in those studies. The data of Fig. 6 and supplementary material S4A,B provide an explanation for the significantly higher extent of TDP-43-positive aggregate formation in MG132-treated N2a cells containing an excess of the full-length TDP-43, whether it is wild-type or the caspase 3-resistant D89A mutant form (Figs 4B, 5B). In other words, 3.6×10^{-5} pmole/cell of the TDP-25 fragment, as generated from the endogenous TDP-43 by MG132-induced caspase 3-cleavage, is sufficient and necessary, as a seed, for effective TDP-43-positive aggregate formation in cells transfected with pMyc-hTDP-43 or pMyc-hTDP-43 (D89A).

With respect to the requirement of an excess of full-length TDP-43, in addition to the TDP-25 seed, to form the TDP-43-positive aggregates, it could be estimated that a total of 8.6×10^{-4} pmole/cell of the full-length TDP-43, or a ~2.7-fold increase in the amount of the endogenous TDP-43 in a normal cell, would be sufficient. Importantly, this level of elevation is similar to or less than those found in pathogenic samples from FTLD-TDP (Chen-Plotkin et al., 2008) and ALS-TDP (Kabashi et al., 2008; Weihl et al., 2008) patients. Furthermore, transgenic animals with overexpression of TDP-43 often develop disease phenotypes that mimic TDP-43 proteinopathies (Ayala et al., 2005; Hanson et al., 2010; Lin et al., 2011; Tsai et al., 2010; Wegorzewska et al., 2009; Wils et al., 2010). For instance, a 2–3-fold increase of full-length TDP-43 in the forebrain of a CamKII-directed transgenic mouse model develops FTLD-TDP-like phenotypes, which are accompanied by elevated levels of insoluble TDP-43 and TDP-35 and TDP-25 fragments, and formation of cytosolic TDP-43-positive aggregates (Tsai et al., 2010). Given that the mere presence of an excess of the full-length TDP-43 does not lead to the formation of TDP-43-positive inclusions (Fig. 5; also see Dormann et al., 2009; Kleinberger et al., 2010; Nonaka et al., 2009b; Tsai et al., 2010), we suggest that an age-dependent process generating a threshold level of the TDP-25 seed is also required for the development of the pathogenic phenotypes of TDP-43 proteinopathies, in particular the formation of the cytosolic TDP-43-positive aggregates, in patients and in transgenic animals with an elevated level of TDP-43.

In summary, a comprehensive study has been carried out regarding the degradation pathways of TDP-43 under normal conditions and the formation of cytosolic TDP-43-positive aggregates when the homeostasis of TDP-43 is dis-regulated. Although the current analysis is only semi-quantitative in certain aspects, for example, the estimation of the minimal amount of TDP-25 fragment as a seed of TDP-43-positive aggregate formation, the results of the study, as depicted in the model of Fig. 7, provide further insights and logical explanations regarding several unsettled points of the metabolism and mis-metabolism of TDP-43. They should further our understanding of the causative roles of elevated full-length TDP-43 and the TDP-25 fragment in TDP-43 pathogenesis.

MATERIALS AND METHODS

Cell culture and DNA and siRNA transfection

Neuro 2a (N2a) cells were cultured in Eagle's minimum essential medium, whereas 293T cells was cultured in Dulbecco's modified Eagle's medium (Invitrogen, Carlsbad, CA), supplemented with 10% (vol/vol) fetal calf serum and penicillin-streptomycin (Invitrogen). DNA and siRNA transfection of N2a and 293T cells was carried out with Lipofectamine 2000 (Invitrogen) according to the manufacturer's instructions.

Plasmid constructs

The cDNA of human hTDP-43 (NM_007375.3) was cloned into BamHI/XhoI restriction sites of pcDNA3.1/Myc-His A vector or into the HindIII/KpnI restriction sites of pEGFP-C1 vector (Invitrogen). For generation of the different hTDP-43 fusion polypeptides, different sets of DNA primer pairs were used to PCR amplify the hTDP-43 coding sequence. The sequences of the different sets of DNA primers used for PCR amplification are as follows: pcDNA3.1/Myc-His-A-hTDP-43 (pMyc-hTDP-43) forward primer, 5′-CGGGATCCCGATGTCTGAATATA-TTCGGGT-3′ and reverse primer 5′-CTTCTCGAGCATTCCCCAG-CCAGA-3′. The PCR product was subcloned into the pcDNA.3.1/Myc-His A plasmid (Invitogen) using restriction sites BamHI and XhoI to generate pcDNA3.1/Myc-His-A-hTDP-43 pcDNA3.1/Myc-His-A-hTDP-25 (pMyc-hTDP-25) (amino acids 175–414) truncated mutant forward primer 5′-CGGGATCCCGATGAATTCTAAGCAAAGCCAA-3′ and reverse primer 5′-CTTCTCGAGCATTCCCCAGCCAGA−3′. The PCR product was subcloned into the pcDNA.3.1/Myc-His A plasmid (Invitogen) using restriction sites BamHI and XhoI to generate pcDNA3.1/Myc-His-A-hTDP-25. pGFP-C1-hTDP-43 (pGFP-hTDP-43) forward primer 5′-CGGAAGCTTATGTCTGAATATATTCGGGT-3′ and reverse primer 5′-CAGGTACCATCATTCCCCAGCCAGA-3′. The PCR product was subcloned into the pEGFP-C1 plasmid (Invitogen) using restriction sites HindIII and KpnI to generate pGFP-C1-hTDP-43.

Site-directed mutants (see below) were generated using the plasmids pcDNA3.1/Myc-His-A-hTDP-43 and pGFP-C1-hTDP-43 as templates. Site-directed mutagenesis (QuikChange kit; Stratagene, La Jolla, CA) was used to create sets of missense mutations for the current study [D89A and QV/AA (Q134A/V135A)]. The sequences of the mutagenized oligonucleotides were as follows: hTDP-43 (QV/AA) mutant, 5′- AGAA-GTTCTTATGGTGGCAGCAAAGAAAGATCTTAAGA-3′; hTDP-43 (D89A) mutant, 5′-AATGGATGAGACAGCAGCTTCATCAGCAG-3′. pEF-HA-Ub was a kind gift from Ying Li, University of California, Irvine, CA.

siRNA-mediated knockdown of mouse LAMP-2A

Mouse LAMP-2A mRNA knockdown in N2a cells was achieved using the specific LAMP-2A siRNA oligonucleotides (Invitrogen). The sequence of the region targeted by the siRNA in the exon 8a of the LAMP-2A gene was 5′-GACTGCAGTGCAGATGAAG-3′ (Massey et al., 2006). A non-targeting negative control siRNA was used to assess the non-specific effect of the siRNA delivery. N2a cells were transfected with 50 nM or 100 nM of the RNA oligonucleotides by Lipofectamine 2000 (Invitrogen) and then analyzed at 48 h post-transfection. The mRNA levels of LAMP-2A, -2B and -2C were

confirmed by RT-PCR using specific primers (Massey et al., 2006): LAMP-2A, 5′-GCAGTGCAGATGAAGACAAC-3′ and 5′-AGTATGATGGCGCTTGAGAC-3′; LAMP-2B, 5′-GGTGCTGGTCTTTCAGGCTTGATT-3′ and 5′-ACCACCCAATCTAAGAGCAGGACT-3′; LAMP-2C, 5′-ATGTGCTGCTGACTCTGACCTCAA-3′ and 5′-TGGAAGCACGAGACTGGCTTGATT-3′; and actin, 5′-AAGGACTCCTATAGTGGGTGACGA-3′ and 5′-ATCTTCTCCATGTCGTCCCAGTTG-3′.

Reagents, recombinant TDP-43 protein and antibodies

Cycloheximide, MG132, 3-methyladenine (3MA) and Z-VAD-FMK were all purchased from Sigma-Aldrich (St Louis, MO). Ammonium chloride (NH_4Cl) was from Merck (Darmstadt, Germany). The following antibodies were used for western blotting: rabbit polyclonal anti-TDP-43 used as indicated in the figure legends (the epitope is amino acids 1–260, Genetex, Irvine, CA, USA and Proteintech Group Inc., Chicago, IL; 1:2000, recognizes human and mouse species), rabbit polyclonal anti-TDP-43 used in Fig. 5A and supplementary material Fig. S4B (the epitope is amino acids 350–414, #ab41881, Abcam, Cambridge, MA, 1:1000, recognizes human and mouse species), mouse monoclonal anti-Myc (Milliport, Bedford, MA, 1:3000), mouse monoclonal anti-α-tubulin (clone B-5-1-2, Sigma-Aldrich, 1:5000), rabbit polyclonal anti-LC3 (Sigma-Aldrich, 1:1000), rabbit polyclonal anti-p62 (Genetex, 1:1000), mouse monoclonal anti-Hsc70 (clone 13D3, Abcam, 1:5000), rabbit polyclonal anti-LAMP-2A (clone ab18528; Abcam, 1:1000). Note that LAMP-2 has three distinct isoforms, LAMP-2A, LAMP-2B and LAMP-2C which are expressed in different tissues and differ in sequences at the extreme C-terminus. The anti-LAMP-2A antibody we used was specific for LAMP-2A protein. Secondary antibodies were horseradish-peroxidase-coupled goat anti-mouse or goat anti-rabbit IgG (Genetex, 1:30,000). Purified recombinant amino acids 252–414 of human TDP-43 (TDP-18) from *E. coli* was a kind gift from Joseph Jen-Tse Huang (Institute of Chemistry, Academia Sinica, Taiwan).

Preparation of cell extracts and immunoblotting

Cultured cells were washed twice in PBS and pelleted at 1000 ***g*** for 5 min. To prepare the total cell extracts, the cell pellets were directly lysed in the urea buffer {7 M urea, 2 M thiourea, 4% 3-[(3-Cholamidopropyl) dimethylammonio]-1-propanesulfonate (CHAPS), 30 mM Tris-HCl pH 8.5} (Sigma-Aldrich). For preparation of RIPA-soluble and insoluble materials (Winton et al., 2008) the cell pellets were first lysed in the RIPA buffer (50 mM Tris-HCl pH 8.0, 150 mM NaCl, 1% NP-40, 0.5% sodium deoxycholate, 0.1% sodium dodecyl sulfate) freshly supplemented with complete EDTA-free protease inhibitor cocktail (Roche Applied Science, Laval, QC, CA) and phosphatase inhibitors (10 mM NaF and 1 mM Na_3VO_4) (Sigma-Aldrich). The protein concentrations of the lysates were determined by Bio-rad protein assay (Biorad, Marnes-la-Coquette, France) and then the lysates were centrifuged at 4℃ for 15 min at 13,800 ***g***. The supernatants containing the RIPA soluble material (S) were transferred into new tubes and boiled in SDS-PAGE sample buffer. The RIPA-insoluble pellets were washed twice in the lysis buffer, re-sonicated and re-centrifuged. The washed pellets (U) were finally dissolved in the urea buffer, sonicated and supplemented with SDS-PAGE sample buffer without boiling. The soluble proteins and insoluble proteins were run on SDS-PAGE gels and transferred onto polyvinylidene difluoride membranes (Immobilon-P, Millipore). After blocking for 1 h in the blocking buffer (5% non-fat dried milk in Tris-buffered saline with 0.1% Tween-20), the membranes were stained with the primary antibodies at 4℃ overnight and then the secondary antibodies at room temperature for 1 h. The bound antibodies were detected by using the chemiluminescence western blotting detection reagent ECL (Amersham Pharmacia Biotech, Piscataway, NJ).

Measurement of the stability of TDP-43 protein

The half-life of TDP-43 protein was analyzed by two different assays. In the cyclohexamide chase assay, transfected or untransfected N2a cells were treated with cycloheximide (20 μg/ml) to inhibit further protein synthesis, and harvested at the indicated time points. TDP-43 protein was analyzed by western blotting and the intensities of the TDP-43 protein bands were quantified, relative to the internal control of α-tubulin, using AlphaEaseFC software. In the [^{35}S]methionine pulse-chase assay, the transfected cells were starved in cysteine and methionine-free medium for 1 h. This was followed by metabolic labeling of the cells with 200 μCi/ml [^{35}S]methionine for 3 h and chased in the regular medium for various time points. The exogenous Myc-tagged TDP-43 proteins were immunoprecipitated with anti-Myc antibody and analyzed by SDS-PAGE and autoradiography. The protein half-life of each TDP-43 species was fitted to the equation of the regression line, $y=ax+b$, obtained from each group where y is the ratio of relative protein levels and x is the time in hours (h).

Co-immunoprecipitation

The interaction between Hsc70 protein and Myc–hTDP-43 was studied by co-immunoprecipitation analysis of extracts prepared from 293T cells transiently transfected with one or more of the plasmids pEF-HA vector, pHA-Ub, pcDNA.3.1/Myc-His A vector, pMyc-hTDP-43 and pMyc-hTDP-43 (D89A). 293T cells at 48 h post-transfection were lysed in the isotonic buffer (10 mM Tris-HCl pH 7.5, 150 mM NaCl, protease inhibitor mixture). After centrifugation at 1400 ***g*** for 5 min at 4℃, the supernatants were pre-cleaned with 50% protein A beads in the isotonic buffer for 30 min at 4℃ and then incubated with anti-Myc at 4℃ overnight. The immunoprecipitates bound to the protein-A–Sepharose beads were washed, boiled and analyzed by western blotting using anti-Hsc70 and anti-TDP-43 antibody.

Immunofluorescence staining and confocal microscopy

N2a cells grown on glass coverslips were transfected with indicated plasmids. At 48 h post-transfection, the cells were treated with different inhibitors or drugs for different periods of time. The cells were fixed with 4% ice-cold paraformaldehyde at 4℃ for 20 min and then permeabilized with PBS with 0.5% Triton X-100 for 7 min at room temperature. After blocking with 10% donkey serum for 1 h at room temperature, the cells were incubated overnight at 4℃ with the rabbit anti-TDP-43 (1:200), mouse anti-Myc (1:500), mouse anti-HuR (Santa Cruz, Texas, USA, 1:100) or rabbit anti-TIA1 (Santa Cruz Biotechnology, Texas, TX; 1:100). After washing, the cells were incubated at room temperature for 1.5 h with DAPI (1:500) (Invitrogen) plus Alexa-Fluor-488-conjugated goat anti-rabbit or Alexa-Fluor-488-conjugated goat anti-mouse IgG secondary antibody (1:500), or plus Alexa-Fluor-546-conjugated goat anti-rabbit or Alexa-Fluor-546-conjugated goat anti-mouse IgG secondary antibody (1:500) (Invitrogen). The images were examined on a Zeiss LSM 710 confocal microscope (Thornwood, NY).

Acknowledgements

We thank Joseph Huang (Institute of Chemistry, Academia Sinica) for his generous gift of purified recombinant human TDP-18 fragment. We thank Ying Li (UC Irvine) for his generous gift of pEF-HA-Ub plasmid. The expertise helps of Sue-Ping Lee and Shu-Mei Huang in the Microscopy Core at IMB are greatly appreciated.

Competing interests

The authors declare no competing interests.

Author contributions

C.C.H. executed most of the experiments and analyzed the data. J.K. performed data analysis and conceived of the study. P.M. performed the [^{35}S]methionine pulse-chase assay experiments. J.T.H. contributed to the purified TDP-18 protein experiments. K.H.L. and J.K.H. participated in its design and coordination and edited the manuscript. C.K.S. conceived, wrote and edited this manuscript. All authors read and approved the final manuscript.

Funding

This work was supported in part by the National Science Council, Taiwan [grant number NSC102-2321-B-001-009]; Taipei Medical University [grant number 12310-0149G]; and by a Frontier of Science grant from the National Science Council and a Senior Investigator Award from the Academia Sinica, Taipei, Taiwan.

Supplementary material

Supplementary material available online at
http://jcs.biologists.org/lookup/suppl/doi:10.1242/jcs.136150/-/DC1

References

Arai, T., Hasegawa, M., Akiyama, H., Ikeda, K., Nonaka, T., Mori, H., Mann, D., Tsuchiya, K., Yoshida, M., Hashizume, Y. et al. (2006). TDP-43 is a component of ubiquitin-positive tau-negative inclusions in frontotemporal lobar degeneration and amyotrophic lateral sclerosis. *Biochem. Biophys. Res. Commun.* **351**, 602-611.

Avendaño-Vázquez, S. E., Dhir, A., Bembich, S., Buratti, E., Proudfoot, N. and Baralle, F. E. (2012). Autoregulation of TDP-43 mRNA levels involves interplay between transcription, splicing, and alternative polyA site selection. *Genes Dev.* **26**, 1679-1684.

Ayala, Y. M., Pantano, S., D'Ambrogio, A., Buratti, E., Brindisi, A., Marchetti, C., Romano, M. and Baralle, F. E. (2005). Human, Drosophila, and C.elegans TDP43: nucleic acid binding properties and splicing regulatory function. *J. Mol. Biol.* **348**, 575-588.

Ayala, Y. M., De Conti, L., Avendaño-Vázquez, S. E., Dhir, A., Romano, M., D'Ambrogio, A., Tollervey, J., Ule, J., Baralle, M., Buratti, E. et al. (2011). TDP-43 regulates its mRNA levels through a negative feedback loop. *EMBO J.* **30**, 277-288.

Baloh, R. H. (2011). TDP-43: the relationship between protein aggregation and neurodegeneration in amyotrophic lateral sclerosis and frontotemporal lobar degeneration. *FEBS J.* **278**, 3539-3549.

Bates, G. (2003). Huntingtin aggregation and toxicity in Huntington's disease. *Lancet* **361**, 1642-1644.

Belizario, J. E., Alves, J., Garay-Malpartida, M. and Occhiucci, J. M. (2008). Coupling caspase cleavage and proteasomal degradation of proteins carrying PEST motif. *Curr. Protein Pept. Sci.* **9**, 210-220.

Bigio, E. H. (2011). TDP-43 variants of frontotemporal lobar degeneration. *J. Mol. Neurosci.* **45**, 390-401.

Bjørkøy, G., Lamark, T., Brech, A., Outzen, H., Perander, M., Overvatn, A., Stenmark, H. and Johansen, T. (2005). p62/SQSTM1 forms protein aggregates degraded by autophagy and has a protective effect on huntingtin-induced cell death. *J. Cell Biol.* **171**, 603-614.

Boillée, S., Vande Velde, C. and Cleveland, D. W. (2006). ALS: a disease of motor neurons and their nonneuronal neighbors. *Neuron* **52**, 39-59.

Braun, R. J., Sommer, C., Carmona-Gutierrez, D., Khoury, C. M., Ring, J., Büttner, S. and Madeo, F. (2011). Neurotoxic 43-kDa TAR DNA-binding protein (TDP-43) triggers mitochondrion-dependent programmed cell death in yeast. *J. Biol. Chem.* **286**, 19958-19972.

Caccamo, A., Majumder, S., Deng, J. J., Bai, Y., Thornton, F. B. and Oddo, S. (2009). Rapamycin rescues TDP-43 mislocalization and the associated low molecular mass neurofilament instability. *J. Biol. Chem.* **284**, 27416-27424.

Che, M. X., Jiang, Y. J., Xie, Y. Y., Jiang, L. L. and Hu, H. Y. (2011). Aggregation of the 35-kDa fragment of TDP-43 causes formation of cytoplasmic inclusions and alteration of RNA processing. *FASEB J.* **25**, 2344-2353.

Chen-Plotkin, A. S., Geser, F., Plotkin, J. B., Clark, C. M., Kwong, L. K., Yuan, W., Grossman, M., Van Deerlin, V. M., Trojanowski, J. Q. and Lee, V. M. (2008). Variations in the progranulin gene affect global gene expression in frontotemporal lobar degeneration. *Hum. Mol. Genet.* **17**, 1349-1362.

Chen-Plotkin, A. S., Lee, V. M. and Trojanowski, J. Q. (2010). TAR DNA-binding protein 43 in neurodegenerative disease. *Nat. Rev. Neurol.* **6**, 211-220.

Cheong, H., Lindsten, T., Wu, J., Lu, C. and Thompson, C. B. (2011). Ammonia-induced autophagy is independent of ULK1/ULK2 kinases. *Proc. Natl. Acad. Sci. USA* **108**, 11121-11126.

Cohen, T. J., Lee, V. M. and Trojanowski, J. Q. (2011). TDP-43 functions and pathogenic mechanisms implicated in TDP-43 proteinopathies. *Trends Mol. Med.* **17**, 659-667.

Cuervo, A. M. and Dice, J. F. (2000). Regulation of lamp2a levels in the lysosomal membrane. *Traffic* **1**, 570-583.

Cuervo, A. M., Stefanis, L., Fredenburg, R., Lansbury, P. T. and Sulzer, D. (2004). Impaired degradation of mutant alpha-synuclein by chaperone-mediated autophagy. *Science* **305**, 1292-1295.

De Strooper, B., Vassar, R. and Golde, T. (2010). The secretases: enzymes with therapeutic potential in Alzheimer disease. *Nat. Rev. Neurol.* **6**, 99-107.

DeMartino, G. N. and Slaughter, C. A. (1999). The proteasome, a novel protease regulated by multiple mechanisms. *J. Biol. Chem.* **274**, 22123-22126.

Demontis, S., Rigo, C., Piccinin, S., Mizzau, M., Sonego, M., Fabris, M., Brancolini, C. and Maestro, R. (2006). Twist is substrate for caspase cleavage and proteasome-mediated degradation. *Cell Death Differ.* **13**, 335-345.

Dice, J. F. (2007). Chaperone-mediated autophagy. *Autophagy* **3**, 295-299.

Dormann, D., Capell, A., Carlson, A. M., Shankaran, S. S., Rodde, R., Neumann, M., Kremmer, E., Matsuwaki, T., Yamanouchi, K., Nishihara, M. et al. (2009). Proteolytic processing of TAR DNA binding protein-43 by caspases produces C-terminal fragments with disease defining properties independent of progranulin. *J. Neurochem.* **110**, 1082-1094.

Filimonenko, M., Stuffers, S., Raiborg, C., Yamamoto, A., Malerød, L., Fisher, E. M., Isaacs, A., Brech, A., Stenmark, H. and Simonsen, A. (2007). Functional multivesicular bodies are required for autophagic clearance of protein aggregates associated with neurodegenerative disease. *J. Cell Biol.* **179**, 485-500.

Furukawa, Y., Kaneko, K., Watanabe, S., Yamanaka, K. and Nukina, N. (2011). A seeding reaction recapitulates intracellular formation of Sarkosyl-insoluble transactivation response element (TAR) DNA-binding protein-43 inclusions. *J. Biol. Chem.* **286**, 18664-18672.

Hanson, K. A., Kim, S. H., Wassarman, D. A. and Tibbetts, R. S. (2010). Ubiquilin modifies TDP-43 toxicity in a Drosophila model of amyotrophic lateral sclerosis (ALS). *J. Biol. Chem.* **285**, 11068-11072.

Hasegawa, M., Nonaka, T., Tsuji, H., Tamaoka, A., Yamashita, M., Kametani, F., Yoshida, M., Arai, T. and Akiyama, H. (2011). Molecular dissection of TDP-43 proteinopathies. *J. Mol. Neurosci.* **45**, 480-485.

Hashimoto, M., Rockenstein, E., Crews, L. and Masliah, E. (2003). Role of protein aggregation in mitochondrial dysfunction and neurodegeneration in Alzheimer's and Parkinson's diseases. *Neuromolecular Med.* **4**, 21-36.

Hatem, C. L., Gough, N. R. and Fambrough, D. M. (1995). Multiple mRNAs encode the avian lysosomal membrane protein LAMP-2, resulting in alternative transmembrane and cytoplasmic domains. *J. Cell Sci.* **108**, 2093-2100.

Hu, Y. L., DeLay, M., Jahangiri, A., Molinaro, A. M., Rose, S. D., Carbonell, W. S. and Aghi, M. K. (2012). Hypoxia-induced autophagy promotes tumor cell survival and adaptation to antiangiogenic treatment in glioblastoma. *Cancer Res.* **72**, 1773-1783.

Igaz, L. M., Kwong, L. K., Xu, Y., Truax, A. C., Uryu, K., Neumann, M., Clark, C. M., Elman, L. B., Miller, B. L., Grossman, M. et al. (2008). Enrichment of C-terminal fragments in TAR DNA-binding protein-43 cytoplasmic inclusions in brain but not in spinal cord of frontotemporal lobar degeneration and amyotrophic lateral sclerosis. *Am. J. Pathol.* **173**, 182-194.

Igaz, L. M., Kwong, L. K., Chen-Plotkin, A., Winton, M. J., Unger, T. L., Xu, Y., Neumann, M., Trojanowski, J. Q. and Lee, V. M. (2009). Expression of TDP-43 C-terminal fragments in vitro recapitulates pathological features of TDP-43 proteinopathies. *J. Biol. Chem.* **284**, 8516-8524.

Iwata, A., Riley, B. E., Johnston, J. A. and Kopito, R. R. (2005). HDAC6 and microtubules are required for autophagic degradation of aggregated huntingtin. *J. Biol. Chem.* **280**, 40282-40292.

Johnson, B. S., McCaffery, J. M., Lindquist, S. and Gitler, A. D. (2008). A yeast TDP-43 proteinopathy model: Exploring the molecular determinants of TDP-43 aggregation and cellular toxicity. *Proc. Natl. Acad. Sci. USA* **105**, 6439-6444.

Ju, J. S., Fuentealba, R. A., Miller, S. E., Jackson, E., Piwnica-Worms, D., Baloh, R. H. and Weihl, C. C. (2009). Valosin-containing protein (VCP) is required for autophagy and is disrupted in VCP disease. *J. Cell Biol.* **187**, 875-888.

Kabashi, E., Valdmanis, P. N., Dion, P., Spiegelman, D., McConkey, B. J., Vande Velde, C., Bouchard, J. P., Lacomblez, L., Pochigaeva, K., Salachas, F. et al. (2008). TARDBP mutations in individuals with sporadic and familial amyotrophic lateral sclerosis. *Nat. Genet.* **40**, 572-574.

Kanazawa, M., Kakita, A., Igarashi, H., Takahashi, T., Kawamura, K., Takahashi, H., Nakada, T., Nishizawa, M. and Shimohata, T. (2011). Biochemical and histopathological alterations in TAR DNA-binding protein-43 after acute ischemic stroke in rats. *J. Neurochem.* **116**, 957-965.

Kim, S. H., Shi, Y., Hanson, K. A., Williams, L. M., Sakasai, R., Bowler, M. J. and Tibbetts, R. S. (2009). Potentiation of amyotrophic lateral sclerosis (ALS)-associated TDP-43 aggregation by the proteasome-targeting factor, ubiquilin 1. *J. Biol. Chem.* **284**, 8083-8092.

Kirkin, V., McEwan, D. G., Novak, I. and Dikic, I. (2009). A role for ubiquitin in selective autophagy. *Mol. Cell* **34**, 259-269.

Kleinberger, G., Wils, H., Ponsaerts, P., Joris, G., Timmermans, J. P., Van Broeckhoven, C. and Kumar-Singh, S. (2010). Increased caspase activation and decreased TDP-43 solubility in progranulin knockout cortical cultures. *J. Neurochem.* **115**, 735-747.

Kuusisto, E., Suuronen, T. and Salminen, A. (2001). Ubiquitin-binding protein p62 expression is induced during apoptosis and proteasomal inhibition in neuronal cells. *Biochem. Biophys. Res. Commun.* **280**, 223-228.

Kwong, L. K., Neumann, M., Sampathu, D. M., Lee, V. M. and Trojanowski, J. Q. (2007). TDP-43 proteinopathy: the neuropathology underlying major forms of sporadic and familial frontotemporal lobar degeneration and motor neuron disease. *Acta Neuropathol.* **114**, 63-70.

Lagier-Tourenne, C., Polymenidou, M. and Cleveland, D. W. (2010). TDP-43 and FUS/TLS: emerging roles in RNA processing and neurodegeneration. *Hum. Mol. Genet.* **19 R1**, R46-R64.

Lansbury, P. T. and Lashuel, H. A. (2006). A century-old debate on protein aggregation and neurodegeneration enters the clinic. *Nature* **443**, 774-779.

Lee, E. B., Lee, V. M. and Trojanowski, J. Q. (2012). Gains or losses: molecular mechanisms of TDP43-mediated neurodegeneration. *Nat. Rev. Neurosci.* **13**, 38-50.

Lin, M. J., Cheng, C. W. and Shen, C. K. (2011). Neuronal function and dysfunction of Drosophila dTDP. *PLoS ONE* **6**, e20371.

Liu, H., Wang, P., Song, W. and Sun, X. (2009). Degradation of regulator of calcineurin 1 (RCAN1) is mediated by both chaperone-mediated autophagy and ubiquitin proteasome pathways. *FASEB J.* **23**, 3383-3392.

Massey, A. C., Kaushik, S., Sovak, G., Kiffin, R. and Cuervo, A. M. (2006). Consequences of the selective blockage of chaperone-mediated autophagy. *Proc. Natl. Acad. Sci. USA* **103**, 5805-5810.

McGrath, M. E. (1999). The lysosomal cysteine proteases. *Annu. Rev. Biophys. Biomol. Struct.* **28**, 181-204.

Mishra, M., Paunesku, T., Woloschak, G. E., Siddique, T., Zhu, L. J., Lin, S., Greco, K. and Bigio, E. H. (2007). Gene expression analysis of frontotemporal lobar degeneration of the motor neuron disease type with ubiquitinated inclusions. *Acta Neuropathol.* **114**, 81-94.

Mizushima, N., Yoshimori, T. and Levine, B. (2010). Methods in mammalian autophagy research. *Cell* **140**, 313-326.

Neumann, M. (2009). Molecular neuropathology of TDP-43 proteinopathies. *Int. J. Mol. Sci.* **10**, 232-246.

Neumann, M., Sampathu, D. M., Kwong, L. K., Truax, A. C., Micsenyi, M. C., Chou, T. T., Bruce, J., Schuck, T., Grossman, M., Clark, C. M. et al. (2006).

Ubiquitinated TDP-43 in frontotemporal lobar degeneration and amyotrophic lateral sclerosis. *Science* **314**, 130-133.

Nomura, Y., Nagaya, T., Yamaguchi, S., Katunuma, N. and Seo, H. (1999). Cleavage of RXRalpha by a lysosomal enzyme, cathepsin L-type protease. *Biochem. Biophys. Res. Commun.* **254**, 388-394.

Nonaka, T., Arai, T., Buratti, E., Baralle, F. E., Akiyama, H. and Hasegawa, M. (2009a). Phosphorylated and ubiquitinated TDP-43 pathological inclusions in ALS and FTLD-U are recapitulated in SH-SY5Y cells. *FEBS Lett.* **583**, 394-400.

Nonaka, T., Kametani, F., Arai, T., Akiyama, H. and Hasegawa, M. (2009b). Truncation and pathogenic mutations facilitate the formation of intracellular aggregates of TDP-43. *Hum. Mol. Genet.* **18**, 3353-3364.

Pesiridis, G. S., Tripathy, K., Tanik, S., Trojanowski, J. Q. and Lee, V. M. (2011). A ''two-hit'' hypothesis for inclusion formation by carboxyl-terminal fragments of TDP-43 protein linked to RNA depletion and impaired microtubule-dependent transport. *J. Biol. Chem.* **286**, 18845-18855.

Polymenidou, M., Lagier-Tourenne, C., Hutt, K. R., Huelga, S. C., Moran, J., Liang, T. Y., Ling, S. C., Sun, E., Wancewicz, E., Mazur, C. et al. (2011). Long pre-mRNA depletion and RNA missplicing contribute to neuronal vulnerability from loss of TDP-43. *Nat. Neurosci.* **14**, 459-468.

Ravikumar, B., Sarkar, S., Davies, J. E., Futter, M., Garcia-Arencibia, M., Green-Thompson, Z. W., Jimenez-Sanchez, M., Korolchuk, V. I., Lichtenberg, M., Luo, S. et al. (2010). Regulation of mammalian autophagy in physiology and pathophysiology. *Physiol. Rev.* **90**, 1383-1435.

Ross, C. A. and Poirier, M. A. (2004). Protein aggregation and neurodegenerative disease. *Nat. Med.* **10** Suppl, S10-S17.

Ross, C. A. and Poirier, M. A. (2005). Opinion: What is the role of protein aggregation in neurodegeneration? *Nat. Rev. Mol. Cell Biol.* **6**, 891-898.

Rutherford, N. J., Zhang, Y. J., Baker, M., Gass, J. M., Finch, N. A., Xu, Y. F., Stewart, H., Kelley, B. J., Kuntz, K., Crook, R. J. et al. (2008). Novel mutations in TARDBP (TDP-43) in patients with familial amyotrophic lateral sclerosis. *PLoS Genet.* **4**, e1000193.

Saini, A. and Chauhan, V. S. (2011). Delineation of the core aggregation sequences of TDP-43 C-terminal fragment. *ChemBioChem* **12**, 2495-2501.

Schotte, P., Declercq, W., Van Huffel, S., Vandenabeele, P. and Beyaert, R. (1999). Non-specific effects of methyl ketone peptide inhibitors of caspases. *FEBS Lett.* **442**, 117-121.

Sreedharan, J., Blair, I. P., Tripathi, V. B., Hu, X., Vance, C., Rogelj, B., Ackerley, S., Durnall, J. C., Williams, K. L., Buratti, E. et al. (2008). TDP-43 mutations in familial and sporadic amyotrophic lateral sclerosis. *Science* **319**, 1668-1672.

Suzuki, H., Lee, K. and Matsuoka, M. (2011). TDP-43-induced death is associated with altered regulation of BIM and Bcl-xL and attenuated by caspase-mediated TDP-43 cleavage. *J. Biol. Chem.* **286**, 13171-13183.

Tanaka, Y., Guhde, G., Suter, A., Eskelinen, E. L., Hartmann, D., Lüllmann-Rauch, R., Janssen, P. M., Blanz, J., von Figura, K. and Saftig, P. (2000). Accumulation of autophagic vacuoles and cardiomyopathy in LAMP-2-deficient mice. *Nature* **406**, 902-906.

Tanida, I., Minematsu-Ikeguchi, N., Ueno, T. and Kominami, E. (2005). Lysosomal turnover, but not a cellular level, of endogenous LC3 is a marker for autophagy. *Autophagy* **1**, 84-91.

Tsai, K. J., Yang, C. H., Fang, Y. H., Cho, K. H., Chien, W. L., Wang, W. T., Wu, T. W., Lin, C. P., Fu, W. M. and Shen, C. K. (2010). Elevated expression of TDP-43 in the forebrain of mice is sufficient to cause neurological and pathological phenotypes mimicking FTLD-U. *J. Exp. Med.* **207**, 1661-1673.

Urushitani, M., Sato, T., Bamba, H., Hisa, Y. and Tooyama, I. (2010). Synergistic effect between proteasome and autophagosome in the clearance of polyubiquitinated TDP-43. *J. Neurosci. Res.* **88**, 784-797.

Wang, I. F., Wu, L. S., Chang, H. Y. and Shen, C. K. (2008). TDP-43, the signature protein of FTLD-U, is a neuronal activity-responsive factor. *J. Neurochem.* **105**, 797-806.

Wang, X., Fan, H., Ying, Z., Li, B., Wang, H. and Wang, G. (2010). Degradation of TDP-43 and its pathogenic form by autophagy and the ubiquitin-proteasome system. *Neurosci. Lett.* **469**, 112-116.

Wang, I. F., Guo, B. S., Liu, Y. C., Wu, C. C., Yang, C. C., Tsai, K. J. and Shen, C. K. J. (2012). Autophagy activators rescue and alleviate pathogenesis of a mouse model with proteinopathies of the TAR DNA-binding protein 43. *Proc. Natl. Acad. Sci. USA* **109**, 15024-15029.

Wegorzewska, I., Bell, S., Cairns, N. J., Miller, T. M. and Baloh, R. H. (2009). TDP-43 mutant transgenic mice develop features of ALS and frontotemporal lobar degeneration. *Proc. Natl. Acad. Sci. USA* **106**, 18809-18814.

Weihl, C. C., Temiz, P., Miller, S. E., Watts, G., Smith, C., Forman, M., Hanson, P. I., Kimonis, V. and Pestronk, A. (2008). TDP-43 accumulation in inclusion body myopathy muscle suggests a common pathogenic mechanism with frontotemporal dementia. *J. Neurol. Neurosurg. Psychiatry* **79**, 1186-1189.

Welchman, R. L., Gordon, C. and Mayer, R. J. (2005). Ubiquitin and ubiquitin-like proteins as multifunctional signals. *Nat. Rev. Mol. Cell Biol.* **6**, 599-609.

Wils, H., Kleinberger, G., Janssens, J., Pereson, S., Joris, G., Cuijt, I., Smits, V., Ceuterick-de Groote, C., Van Broeckhoven, C. and Kumar-Singh, S. (2010). TDP-43 transgenic mice develop spastic paralysis and neuronal inclusions characteristic of ALS and frontotemporal lobar degeneration. *Proc. Natl. Acad. Sci. USA* **107**, 3858-3863.

Winton, M. J., Igaz, L. M., Wong, M. M., Kwong, L. K., Trojanowski, J. Q. and Lee, V. M. (2008). Disturbance of nuclear and cytoplasmic TAR DNA-binding protein (TDP-43) induces disease-like redistribution, sequestration, and aggregate formation. *J. Biol. Chem.* **283**, 13302-13309.

Wong, J., Zhang, J., Si, X., Gao, G., Mao, I., McManus, B. M. and Luo, H. (2008). Autophagosome supports coxsackievirus B3 replication in host cells. *J. Virol.* **82**, 9143-9153.

Yamashita, T., Hideyama, T., Hachiga, K., Teramoto, S., Takano, J., Iwata, N., Saido, T. C. and Kwak, S. (2012). A role for calpain-dependent cleavage of TDP-43 in amyotrophic lateral sclerosis pathology. *Nat. Commun.* **3**, 1307-1314.

Zhang, Y. J., Xu, Y. F., Dickey, C. A., Buratti, E., Baralle, F., Bailey, R., Pickering-Brown, S., Dickson, D. and Petrucelli, L. (2007). Progranulin mediates caspase-dependent cleavage of TAR DNA binding protein-43. *J. Neurosci.* **27**, 10530-10534.

Zhang, Y. J., Xu, Y. F., Cook, C., Gendron, T. F., Roettges, P., Link, C. D., Lin, W. L., Tong, J., Castanedes-Casey, M., Ash, P. et al. (2009). Aberrant cleavage of TDP-43 enhances aggregation and cellular toxicity. *Proc. Natl. Acad. Sci. USA* **106**, 7607-7612.